JOURNAL OF PETROLOGY | VOLUME 47 | NUMBER 2 | PAGES 277–299 | 2006 | doi:10.1093/petrology/egi075

Petrology and Geochemistry of West Philippine Basin Basalts and Early Palau–Kyushu Arc Volcanic Clasts from ODP Leg 195, Site 1201D: Implications for the Early History of the Izu–Bonin–Mariana Arc

IVAN P. SAVOV[1]*, ROSEMARY HICKEY-VARGAS[2], MASSIMO D'ANTONIO[3], JEFFREY G. RYAN[1] AND PIERA SPADEA[4]

[1]GEOLOGY DEPARTMENT, UNIVERSITY OF SOUTH FLORIDA, TAMPA, FL 33620, USA

[2]DEPARTMENT OF EARTH SCIENCES, FLORIDA INTERNATIONAL UNIVERSITY, MIAMI, FL 33199, USA

[3]DIPARTIMENTO DI SCIENZE DELLA TERRA, UNIVERSITY FEDERICO II, NAPOLI 80138, ITALY, AND OSSERVATORIO VESUVIANO, ISTITUTO NAZIONALE DI GEOFISICA E VULCANOLOGIA, NAPOLI, ITALY

[4]DIPARTIMENTO GEORISORSE E TERRITORIO, UNIVERSITY OF UDINE, UDINE 33100, ITALY

RECEIVED MARCH 17, 2004; ACCEPTED JULY 28, 2005
ADVANCE ACCESS PUBLICATION AUGUST 31, 2005

Site 1201D of Ocean Drilling Program Leg 195 recovered basaltic and volcaniclastic units from the West Philippine Basin that document the earliest history of the Izu–Bonin–Mariana convergent margin. The stratigraphic section recovered at Site 1201D includes 90 m of pillow basalts, representing the West Philippine Basin basement, overlain by 459 m of volcaniclastic turbidites that formed from detritus shed from the Eocene–Oligocene proto-Izu–Bonin–Mariana island arc. Basement basalts are normal mid-ocean ridge basalt (N-MORB), based on their abundances of immobile trace elements, although fluid-mobile elements are enriched, similar to back-arc basin basalts (BABB). Sr, Nd, Pb and Hf isotopic compositions of the basement basalts are similar to those of basalts from other West Philippine Basin locations, and show an overall Indian Ocean MORB signature, marked by high $^{208}Pb/^{204}Pb$ for a given $^{206}Pb/^{204}Pb$ and high $^{176}Hf/^{177}Hf$ for a given $^{143}Nd/^{144}Nd$. Trace element and isotopic differences between the basement and overlying arc-derived volcaniclastics are best explained by the addition of subducted sediment or sediment melt, together with hydrous fluids from subducted oceanic crust, into the mantle source of the arc lavas. In contrast to tectonic models suggesting that a mantle hotspot was a source of heat for the early Izu–Bonin–Mariana arc magmatism, the geochemical data do not support an enriched, ocean island basalt (OIB)-like source for either the basement basalts or the arc volcanic section.

KEY WORDS: *back-arc basalts; Izu–Bonin–Marianas; Philippine Sea; subduction initiation; Ocean Drilling Program Leg 195*

INTRODUCTION

The 'Subduction Factory' experiment represents an effort by geophysicists, geochemists and petrologists to model the processes of element recycling at convergent plate margins. The conceptual framework of such modeling is based on the assumption that there must be a balance between what and how much is added to the Earth's mantle via subduction (slab inputs) and the quantity and composition of island arc lavas, the residual slab and associated forearc and back-arc regions (arc outputs). As summarized by Stern *et al.* (2003), the Izu–Bonin–Mariana (IBM) arc system presents an outstanding opportunity to study the operation of the

*Corresponding author. Present address: Department of Mineral Sciences, Smithsonian Institution, P.O. Box 37012, NHB-119, Washington, DC 20013-7012, USA. Telephone: (202)-633-1799. Fax: (202)-357-2476. E-mail: savovi@si.edu

© The Author 2005. Published by Oxford University Press. All rights reserved. For Permissions, please e-mail: journals.permissions@oxfordjournals.org

Downloaded from http://petrology.oxfordjournals.org/ at Kainan University on March 28, 2015

Subduction Factory at an intra-oceanic convergent margin because:

(1) its history is well constrained;

(2) samples have been obtained of the entire slab inventory (input) including the sedimentary column approaching the trench and the underlying altered oceanic crust (AOC) (Plank & Langmuir, 1998; Kelley *et al.*, 2003);

(3) there is no accretionary prism, so sediments are completely subducted;

(4) there are four opportunities across the arc to sample materials produced by the Subduction Factory (outputs)—the forearc, the active magmatic arc, across-arc seamount chains and back-arc basins.

One major question about the IBM arc is how subduction was initiated, and how arc magmatism (i.e. outputs) has varied in composition over the history of the arc (Hickey-Vargas & Reagan, 1987; Hickey-Vargas, 1989, 1991; Stern *et al.*, 1991; Arculus *et al.*, 1995; Pearce *et al.*, 1999; Reagan *et al.*, 2002). To understand element recycling at a specific convergent margin, we need to know what are the temporal and spatial input–output variations through time. In the IBM arc, fragments of the older Eocene–Oligocene proto-arc are preserved both in the forearc and in the Palau–Kyushu Ridge remnant arc (Fig. 1). One of the most exciting findings of Ocean Drilling Program (ODP) Leg 195 was that the section cored at Site 1201D sampled both West Philippine Basin floor and overlying arc volcanics shed from the Palau–Kyushu Ridge, a situation that is not found in any other locale to date. In this paper we report on the geochemical and isotopic features of this section, including samples from the West Philippine Basin oceanic crust on which the proto-IBM arc was formed, as well as the volcanic products of this early arc (Palau–Kyushu Ridge volcanics).

REGIONAL GEOLOGY AND ODP SITE 1201D

The West Philippine Basin (WPB) opened within the Philippine Sea Plate (PSP) between about 65 Ma and 35 Ma by spreading along the now extinct Central Basin spreading center, which is marked at present by the Central Basin Fault (CBF, Fig. 1). Despite exploration on Deep Sea Drilling Project (DSDP) Legs 7, 31, 58 and 59, and ODP Legs 125, 126 and 195, the tectonic and geochemical evolution of the West Philippine Basin is still debated. Competing hypotheses are that the West Philippine Basin is a trapped fragment of ocean floor (Uyeda & Ben Avraham, 1972), or that it is a back-arc basin associated with the proto-IBM arc (Seno & Maruyama, 1984; Deschamps & Lallemand, 2002). Basalts recovered from the West Philippine Basin floor by DSDP Legs 7, 31, 58 and 59 have both mid-ocean ridge basalt (MORB) and oceanic island basalt (OIB)-like characteristics (Marsh *et al.*, 1980; Mattey *et al.*, 1981; Hickey-Vargas, 1991, 1998*a*, 1998*b*). Normal (N)-MORB-like basalts were found at DSDP Sites 290 and 447 near the Central Basin Fault to the SW of Site 1201D, and enriched (E)-MORB-like basalts were found at DSDP Site 291 in the southern West Philippine Basin. OIB-like basalts were found at DSDP Sites 292, 294 and 446 (Fig. 1). Among the OIB-like basalts, only those from Site 292 are associated with a seamount, the Benham Rise. Thus the geochemical character of West Philippine Basin floor basalts is not linked with bathymetry in a simple way. West Philippine Basin studies are also complicated by the fact that the outcrops are 5–6 km underwater, with the CBF fossil spreading axial valley reaching almost 8 km water depth (Fujioka *et al.*, 1999). One of the principal objectives for drilling at Site 1201D was to study the composition and temporal evolution of the easternmost West Philippine Basin and the bordering Palau–Kyushu Ridge in the context of the proposed Subduction Factory Science Plan (http://www.margins.wustl.edu/SF/I-B-M/IZUBonin.html).

ODP Site 1201D is located in the West Philippine Basin in 5711 m of water, about 100 km west of the Palau–Kyushu Ridge and 450 km north of the CBF (Fig. 1). Early interpretations of the magnetic lineations (Hilde & Lee, 1984) indicated that Site 1201D lies on 49 Ma crust near Chron 21, and formed by NE–SW-directed spreading on the CBF. At about 42 Ma, the spreading rate and direction changed to north–south, and finally stopped at about 35 Ma as volcanism ceased in the early IBM arc (Hussong & Uyeda, 1981). Because the earliest magnetic anomalies in the region pre-date the initiation of subduction at about 50–45 Ma along the IBM arc (Cosca *et al.*, 1998), Hilde & Lee (1984) proposed that the West Philippine Basin initially formed by entrapment of an older North New Guinea or Pacific spreading ridge. More recent bathymetric and magnetic surveys (Okino *et al.*, 1999) have shown that the site lies at a transition from well-defined anomalies south of the Oki–Daito Ridge to more complicated anomalies on the north side, which implies that the crust to the north may have formed at a different spreading center. Analysis of paleolatitude and declination data from the Philippine Sea Plate and its margins suggests that the plate has drifted about 15° to the north and rotated clockwise by up to 90° since the middle Eocene (Hall *et al.*, 1995).

Although the age of the basement in the northern West Philippine Basin has been estimated from magnetic anomalies, paleontological confirmation has been imprecise because of spot coring, core disturbance and poor preservation of microfossils. A goal of the ODP Leg 195 drilling was to obtain an accurate basement age from undisturbed microfossils, magnetostratigraphy or radiometric dating of ash horizons, using modern coring

Downloaded from http://petrology.oxfordjournals.org/ at Kainan University on March 28, 2015

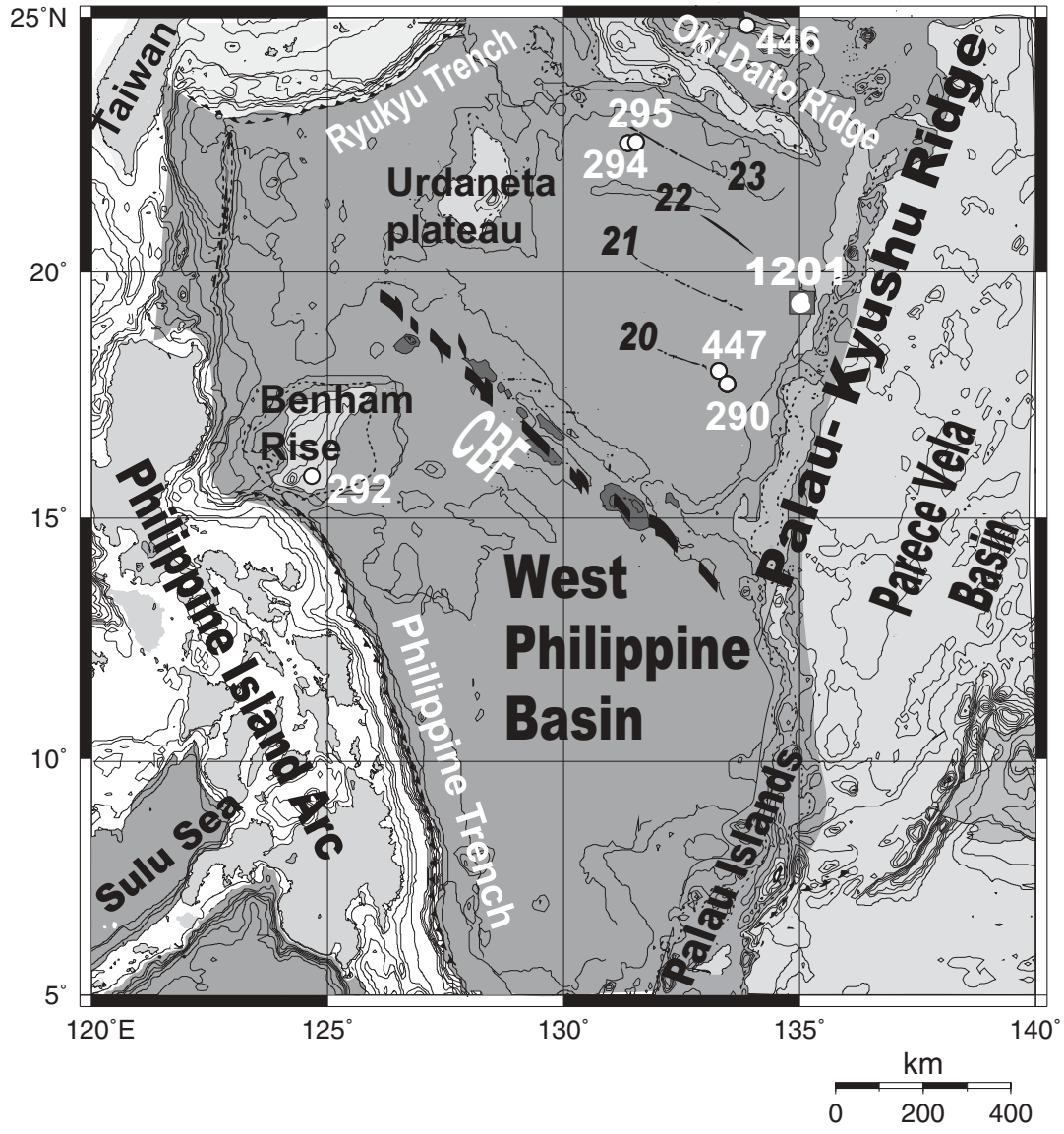

Fig. 1. Location map of ODP Leg 195 Site 1201D. The site was drilled ~100 km west of the Palau–Kyushu Ridge between the Oki Daito Ridge (to the north) and Central Basin Fault (CBF) (to the south). Magnetic anomalies (chrons 20–23) are from Hilde & Lee (1984). Other DSDP sites in the area (290, 292, 294, 295, 446 and 447) are also indicated.

techniques (Shipboard Scientific Party, 2002). Based on 66 core sections Site 1201D yielded 510 m of Miocene to late Eocene sediments, and 90 m of basalt basement (Fig. 2).

The uppermost lithological unit [0–53 m below sea floor (mbsf), Fig. 2] consists of soft pelagic clays, cherts and interbedded sandstones and silty claystones that contain significant amounts of red clay. The underlying lithological unit (53–512 mbsf, Fig. 2) comprises a thick section of interbedded turbidites composed of detrital volcaniclastic material and traces of reef detritus from the Palau–Kyushu remnant arc, which range in size from coarse sandstones and breccias through silty claystone to claystone. The individual turbidite layers range from tens of meters to a few millimeters in thickness.

The topmost (0–29 mbsf) and the lowermost sections (462–509 mbsf) are barren of nannofossils, but moderately preserved nannofossils in the middle section allow the recognition of six biozones spanning NP19/20 to NP25. The turbidites between 53 and 462 mbsf represent an expanded sequence of late Eocene to early Oligocene age (Salisbury *et al.*, 2002). Compared with DSDP drilling results at Sites 290 and 447 (Arculus *et al.*, 1995; Deschamps & Lallemand, 2002) the late Eocene

Downloaded from http://petrology.oxfordjournals.org/ at Kainan University on March 28, 2015

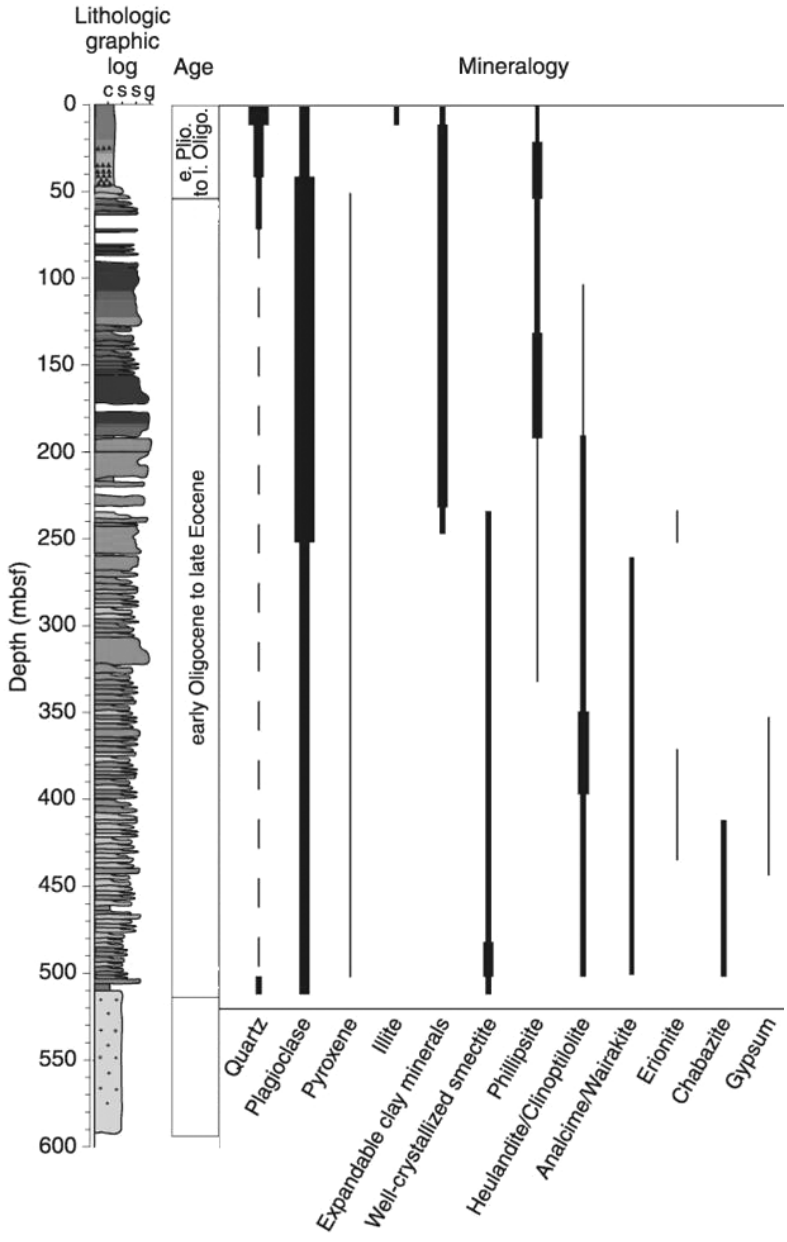

Fig. 2. Major lithological, age and mineralogical variations with depth at ODP Site 1201D. mbsf, meters below sea floor. After Salisbury *et al.* (2002).

sediments (>34·3 Ma) recovered at this site are the oldest so far identified on the sedimentary apron of the Palau–Kyushu Ridge. Sediments at DSDP Site 447 reached a maximum age of Middle Oligocene.

The combined biostratigraphic and paleomagnetic results show that the sedimentation rates were moderate (35 m/Myr) in the late Eocene, then very high (109 m/Myr) in late Eocene–early Oligocene time when the turbidites were being deposited, and then decreased to very low values (3 m/Myr) during the Miocene when the pelagic sediments at the top of the section were being deposited. The two lithostratigraphic units mentioned briefly above have been described in more detail by Salisbury *et al.* (2002).

The 90 m of basement drilled at Site 1201D consist entirely of pillow basalts. Geochemical and thin-section analysis shows that the basalts have been altered, especially at the contact with the overlying sediments, where they show significant Na uptake and depletion in Ca (see also D'Antonio & Kristensen, 2004). Hyaloclastites in the section have been palagonitized and altered to smectite; interpillow sediments recovered from within the upper

Downloaded from http://petrology.oxfordjournals.org/ at Kainan University on March 28, 2015

10 m of the volcanic basement contain marine microfossils, indicating eruption in a marine environment. Magnetic inclinations in the basaltic basement are shallow and indicate that during the Eocene the PSP was near the Equator (Salisbury *et al.*, 2002).

From the data provided above, it can be concluded that the basement at Site 1201D formed near the Equator by submarine eruption before 34·3 Ma. The absence of calcareous nannofossils and the presence of siliceous microfossils in the inter-pillow sediments and pelagic sediments immediately overlying the basement suggest that the basement formed in a deep-water environment below the carbonate compensation depth (CCD) (Shipboard Scientific Party, 2002).

Before the opening of the Parece–Vela and Shikoku Basins at ~30 Ma (Okino *et al.*, 1999), the Palau–Kyushu Ridge and the Izu–Bonin–Mariana arc constituted a single volcanic arc (~48 to 35 Ma; Arculus *et al.*, 1995; Cosca *et al.*, 1998; Deschamps & Lallemand, 2002; Stern *et al.*, 2003). In the late Eocene and early Oligocene (from ~35 to 30 Ma), pelagic sedimentation at Site 1201D became mixed with, and was finally overwhelmed by increasingly thick, coarse and energetic turbidites, composed of arc-derived volcaniclastics and reef detritus. The composition and timing of the turbidites are consistent with a source to the east in the Palau–Kyushu remnant arc.

Between the late Oligocene and early Pliocene, the deposition of turbidites came to an end and pelagic sedimentation resumed at Site 1201D. The volcanism moved to the east (to the West Mariana Ridge and current Mariana island arc) in response to plate reorganization (Deschamps & Lallemand, 2002) and the Palau–Kyushu Ridge subsided.

SAMPLE SELECTION AND ANALYTICAL METHODS

Samples representative of both volcanic clasts in turbidites and basalts from the basement cored at Site 1201D were selected for geochemical and isotopic analysis, based on petrographic examination and the results of shipboard major and trace element analysis. Major and trace element analyses of some 30 basalt samples were performed by inductively coupled plasma atomic emission spectrometry (ICP-AES) onboard R.V. *JOIDES Resolution* using a JY 2000 system (Shipboard Scientific Party, 2002) (Table 1). Sample solutions were analyzed for Si, Al, Mg, Mn, Fe, Ca, Na, K, Ti, Sr, Ba, Zr, Y, P, Cr, Ni, Sc, V, Zn and Cu. Samples (0·1 g) of the powdered and dried sample chips were mixed with 0·4 g of $LiBO_2$ flux in Au–Pt crucibles. The samples were then fused at 1050°C for 12 min and the resulting glass beads were dissolved in 50 ml of 10% HNO_3 (dilution of 500). Concentrations of the elements of interest were reproducible, based on monitoring by replicates of the certified USGS and JGS standards AGV-1, BIR-1, BHVO-2, W-2 and JGb-1. Precision was generally better than 5%. Replicate analyses of basalt sample solutions showed accuracy to be 5–10%. Clasts were mechanically separated from the turbidites. Major elements, loss on ignition (LOI) and some trace elements in the clasts were measured by ICP-AES using the JY 70 system at Florida International University, following the procedures described by Hickey-Vargas (1998*a*).

Based on major element analyses of basement rocks analyzed aboard ship, LOI values and petrographic inspection for alteration, 14 basement rocks and three clasts were selected for high-precision trace element analysis by ICP-mass spectrometry (ICP-MS) and isotopic analysis. Because samples analyzed aboard ship were powdered in tungsten carbide, new powder splits were prepared for the trace element and isotopic analysis using alumina or agate vessels. For ICP-MS analysis, samples were dissolved by HF–HNO_3 digestion and analyzed for rare earth elements (REE), Y, Sr, Rb, Cs, Pb, As, Sb, U, Th, Nb, Ta, Hf, Zr, Sc, V, Ga, Cu, Zn, Li and Be by ICP-MS using the VG Elemental II system of the Department of Earth Sciences at Boston University, Boston, MA. Techniques and reproducibility have been reported by Johnson & Plank (1999) and Kelley *et al.* (2003).

Nine basement basalts and three clasts were selected for isotopic analysis based on freedom from alteration, as judged from trace element analyses, low LOI, and petrographic inspection. Powdered samples were leached in cold 0·1N HCl before dissolution to remove any embedded carbonate and salts. Samples were prepared for Pb isotope analysis at Florida International University and measurements were carried out at the Geochemistry Section of the National High Magnetic Field Laboratory (NHMFL) at Florida State University by thermal ionization mass spectrometry (TIMS) using a Finnigan MAT 262. Measured ratios were normalized to the NBS 981 standard of Todt *et al.* (1993). Repeated runs of NBS-981 and their ±2 SD errors, respectively, are as follows: $^{206}Pb/^{204}Pb$ =16·8865 (2σ = 0·01497); $^{207}Pb/^{204}Pb$ = 15·4260 (2σ = 0·01438) and $^{208}Pb/^{204}Pb$ = 36·4935 (2σ = 0·01421).

The Sr and Nd analyses were carried out on the sample residue after Pb separation, at Osservatorio Vesuviano (Istituto Nazionale di Geofisica e Vulcanologia, Naples, Italy). Sr and Nd were extracted by conventional ion-exchange chromatographic techniques in a clean laboratory. Measurements were made by TIMS on a ThermoFinnigan Triton TI multicollector mass spectrometer running in static mode. The normalization value for fractionation of $^{87}Sr/^{86}Sr$ was $^{86}Sr/^{88}Sr$ = 0·1194; that of $^{143}Nd/^{144}Nd$ was $^{146}Nd/^{144}Nd$ = 0·7219. Instrument errors for determinations of $^{87}Sr/^{86}Sr$ and

Downloaded from http://petrology.oxfordjournals.org/ at Kainan University on March 28, 2015

Table 1: Shipboard ICP-AES major and trace element analyses for basement basalts from ODP Site 1201D

Core & section:	45R-5	46R-1	46R-1	46R-1	46R-2	46R-4	46R-4	46R-5	47R-2	47R-2	47R-3	47R-3	48R-1	48R-2	48R-2
cm interval:	(104–107)	(108–110)	(134–136)	(138–140)	(108–110)	(24–27)	(31–33)	(58–60)	(85–87)	(124–126)	(83–86)	(121–124)	(48–50)	(74–76)	(135–138)
Piece no.:	1	8	10	10	5B	6A	7	4B	10	16	7	13	2C	1D	5C
Depth (mbsf):	509·9	513·98	514·24	514·28	515·48	517·5	517·57	519·34	524·45	524·84	525·91	526·29	532·18	533·18	533·79
wt %															
SiO_2	51·38	47·66	51·76	50·74	50·42	50·76	49·70	49·38	49·78	49·60	49·20	49·45	49·37	49·85	49·35
TiO_2	0·90	0·97	1·02	0·90	0·91	1·01	0·77	0·89	0·91	0·89	0·96	0·94	0·92	0·92	0·92
Al_2O_3	16·27	17·17	16·23	16·19	16·80	17·02	17·29	17·18	16·03	16·36	16·28	16·07	15·62	15·96	15·70
Fe_2O_{3T}	9·15	9·51	9·76	8·83	8·80	10·08	10·53	8·72	9·16	9·10	9·29	10·48	8·99	9·92	10·65
MnO	0·16	0·16	0·15	0·15	0·14	0·16	0·14	0·15	0·14	0·14	0·20	0·20	0·17	0·20	0·22
MgO	6·08	7·38	6·76	7·18	7·68	7·39	5·22	7·87	8·40	8·64	8·08	8·23	8·18	8·52	8·38
CaO	14·05	12·13	7·35	9·69	11·86	7·92	6·67	11·27	9·05	11·01	12·03	13·16	13·15	13·70	13·26
Na_2O	2·83	2·98	5·48	4·00	2·77	4·75	4·73	2·83	3·68	3·15	2·06	2·13	2·09	2·13	2·08
K_2O	0·65	0·89	1·25	1·11	1·13	1·18	2·84	1·14	1·31	1·26	0·48	0·57	0·24	0·26	0·35
P_2O_5	0·19	0·21	0·13	0·20	0·04	0·12	0·06	0·15	0·16	0·22	0·13	0·10	0·09	0·07	0·09
Total	101·65	99·07	99·90	99·00	100·56	100·39	97·95	99·58	98·61	100·37	98·70	101·34	98·82	101·54	100·99
LOI	3·3	5·9	6·5	5·0	5·9	6·6	11·9	5·1	4·9	6·2	1·76	1·83	1	1·4	0·97
Mg-no.	59·89	63·55	60·91	64·62	66·23	62·23	52·71	66·96	67·33	68·09	66·15	63·84	67·18	65·89	63·88
ppm															
Sc	41·9	47·6	48·3	42·6	45·7	46·1	36·0	43·7	46·9	46·4	46·4	42·0	45·1	42·5	41·6
V	237·6	293·9	234·0	242·2	252·9	263·8	98·3	239·9	283·5	279·9	303·6	260·2	277·4	249·6	259·4
Cr	342·4	348·1	359·7	330·2	397·8	363·9	165·0	360·4	351·2	324·2	414·4	409·9	379·5	397·2	407·4
Ni	71·2	—	72·2	73·0	142·4	88·8	—	106·3	—	—	—	—	—	—	—
Sr	109·4	145·7	26·6	64·7	223·3	51·9	41·1	134·4	86·8	103·0	80·9	80·8	77·7	80·1	80·0
Y	26·6	25·8	28·4	23·8	22·7	28·1	9·0	22·9	26·8	24·2	25·7	24·9	23·9	23·2	24·6
Ba	14·5	21·3	26·2	19·7	22·3	24·5	16·7	23·5	26·0	26·0	14·9	12·5	11·5	10·9	10·4
Zr	50·5	50·7	56·7	51·9	52·2	56·4	46·8	48·8	50·6	47·1	47·2	48·2	44·6	46·0	47·1

Downloaded from http://petrology.oxfordjournals.org/ at Kainan University on March 28, 2015

Core & section:	48R-3	48R-4	49R-1	49R-2	49R-2	51R-1	52R-1	53R-1	54R-1	54R-1	54R-2	54R-2	55R-1	55R-1	55R-2
cm interval:	(77–79)	(70–72)	(144–7)	(28–30)	(131–133)	(22–23)	(78–80)	(116–118)	(43–45)	(69–71)	(39–41)	(118–120)	(43–45)	(103–106)	(95–97)
Piece no.:	7C	13	14C	6	14	4	7A	17A	4	9	4C	9	5G	5R	8
Depth (mbsf):	534·71	536·04	542·74	543·08	544·11	554·22	561·48	571·46	579·93	580·19	581·07	581·86	588·53	589·13	590·51
wt %															
SiO_2	50·01	50·79	49·76	50·53	48·35	47·49	50·14	50·01	50·07	50·51	49·54	50·01	50·30	50·32	49·65
TiO_2	0·92	0·91	0·92	0·93	0·88	0·88	0·94	0·95	0·97	1·01	0·94	0·94	0·90	0·91	0·96
Al_2O_3	15·87	15·97	15·97	16·15	15·45	15·38	16·29	16·39	16·61	17·24	16·32	16·44	15·45	15·72	16·43
Fe_2O_{3T}	10·03	10·24	8·66	9·51	8·83	8·29	10·03	10·42	10·64	10·81	10·54	9·62	9·23	9·40	9·95
MnO	0·21	0·21	0·17	0·22	0·19	0·17	0·21	0·22	0·17	0·16	0·23	0·18	0·18	0·18	0·18
MgO	8·71	8·90	8·07	8·81	8·43	7·93	8·31	7·91	6·14	5·83	7·69	7·44	8·34	8·15	6·64
CaO	13·81	13·89	14·06	13·65	13·19	12·16	13·25	13·84	12·95	11·79	13·66	14·11	13·39	13·84	13·17
Na_2O	2·11	2·14	2·02	2·13	1·83	1·82	2·18	1·96	1·85	2·32	2·02	1·98	2·06	2·08	2·58
K_2O	0·18	0·23	0·26	0·30	0·29	0·36	0·48	0·64	1·41	1·49	0·67	0·45	0·18	0·19	0·75
P_2O_5	0·05	0·08	0·09	0·09	0·10	0·05	0·10	0·09	0·14	0·13	0·08	0·09	0·09	0·08	0·12
Total	101·90	103·38	99·97	102·32	97·54	94·53	101·93	102·43	100·97	101·29	101·70	101·26	100·13	100·88	100·44
LOI	1·24	0·85	1·65	1·65	1·58	1·78	1·73	2·31	2·109	3·71	2·25	1·32	2·14	1·89	3·58
Mg-no.	66·14	66·15	67·68	67·56	68·21	68·25	65·07	63·03	56·48	54·79	62·14	63·50	67·01	66·10	60·00
ppm															
Sc	39·5	42·3	41·6	43·7	42·3	43·0	43·6	45·0	45·7	46·0	43·9	43·9	41·6	41·7	48·1
V	246·5	261·2	257·1	259·8	243·9	239·5	270·0	285·8	286·1	323·2	286·7	281·8	247·9	260·4	300·4
Cr	416·8	420·8	426·1	431·8	411·2	398·6	409·5	425·2	437·5	460·3	411·0	436·0	415·4	423·7	420·9
Ni	—	—	130·2	—	—	—	—	—	74·0	90·1	—	94·7	166·7	124·2	88·4
Sr	79·4	79·7	82·1	80·5	78·3	77·7	83·7	81·5	84·6	92·0	81·5	82·1	79·3	79·1	108·7
Y	23·3	24·3	24·0	24·9	23·4	23·6	24·9	25·1	27·9	30·6	24·0	23·4	23·3	23·4	25·3
Ba	10·8	11·6	9·5	11·0	11·4	11·9	11·2	13·5	21·0	21·1	15·2	11·8	11·3	8·2	16·0
Zr	44·5	47·9	47·7	43·9	45·7	43·2	50·1	52·4	50·0	50·9	44·5	46·8	44·8	44·3	48·5

Downloaded from http://petrology.oxfordjournals.org/ at Kainan University on March 28, 2015

$^{143}Nd/^{144}Nd$ are indicated in Table 4 as 2σ of the mean. External precision (2σ) for Sr and Nd isotope ratios from successive replicate measurements of standards was better than 7 ppm for the SRM-987 International Sr Reference Standard (average $^{87}Sr/^{86}Sr = 0{\cdot}710249$; $n = 29$; standard deviation $= 6{\cdot}6 \times 10^{-6}$) and better than 5 ppm for the La Jolla International Reference Nd Standard (average $^{143}Nd/^{144}Nd = 0{\cdot}511850$; $n = 24$; standard deviation $= 8 \times 10^{-6}$). The total blanks for Sr and Nd were negligible for the measured samples during the period of measurements.

Hf isotopic analyses were performed on separate powder splits, using the dissolution and separation techniques described by Bizimis *et al.* (2004). Measurements were made using the hot secondary ionization mass spectrometry technique at NHMFL/Florida State University, following methods described by Bizimis *et al.* (2004). The JMC 475 Hf standard was measured at $0{\cdot}282199 \pm 22$ (2 S.D., $n = 15$) and values are reported relative to the accepted value of 0·282160. Measured total Hf blanks were negligible during the period of measurements.

PETROGRAPHY

Thin sections from the Site 1201D cores were prepared both onboard R.V. *JOIDES Resolution* and onshore, covering all the rock varieties observed in the cores. We examined 45 West Philippine Basin basalts and 15 Palau–Kyushu volcanic clast samples separated from the turbidite sedimentary basement cover.

The West Philippine Basin basement basalts are mostly aphyric to moderately porphyritic (~7% phenocrysts), with phenocrysts of plagioclase, olivine, clinopyroxene, and opaque minerals. A general trend of greater percentage of phenocrysts is observed with increasing core depth. Glass-rich basalts contain microphenocrysts of plagioclase and clinopyroxene arranged in spherulitic textures, but hyalopilitic and branching textures are common as well. The more crystalline basalt varieties have felty, intersertal, intergranular and subophitic textures. The inferred order of crystallization is plagioclase ± olivine, followed by clinopyroxene and later opaque minerals. The degree of alteration and replacement varies significantly as evidenced by the large LOI variations (0·77–11·85%, Table 1). In altered samples, volcanic glass is devitrified to clay minerals and zeolites, plagioclase is commonly replaced by calcite, alkali feldspar and zeolites, and olivine is represented by pseudomorphs of clay minerals, iron oxyhydroxides and calcite (D'Antonio & Kristensen, 2004). Based on shipboard X-ray diffraction analysis, the replacement mineralogy of the Site 1201D basement basalts suggests zeolite-facies metamorphic grade.

The Palau–Kyushu arc-derived clasts are calc-alkaline basalts, basaltic andesites, andesites and dacites. Many of these rocks are highly vesicular (up to 30% vesicles). The dominant phenocryst minerals in the basalts are plagioclase and clinopyroxene in the proportion 60:40, ± orthopyroxene and magnetite, with interstitial brown volcanic glass. Olivine pseudomorphs (up to 10%, now an aggregate of calcite, clay minerals and chlorite) are present in some samples. Alteration is more evident in the basaltic clasts than in the basalt samples from the basement. In some samples, the vesicles are filled with fibrous and/or prismatic zeolite group minerals, and plagioclase phenocrysts are albitized and/or zeolitized [for details, see D'Antonio & Kristensen (2004)].

BULK-ROCK GEOCHEMISTRY

Major and trace elements

Basement section

The upper 20 m of the basaltic section at Site 1201D (Sections 45, 46 and 47-1 and -2, Tables 1 and 2) shows elevated LOI values (average 6·45%), Na_2O (up to 4·7 wt %), and highly variable K_2O (1–3 wt %) and Sr (27–490 ppm) contents. Below this depth, the basalts show diminished signs of seawater alteration and their LOI values stabilize to ~1·8%. The studied samples are in general fairly primitive basalts, with high $Mg/(Mg + \Sigma Fe$ (range 55–68; average 64), MgO contents averaging ~8 wt %, and high Cr (average ~400 ppm) and Ni (average ~110 ppm) contents (Tables 1 and 2). The basement samples also have low mean TiO_2 (~0·9 wt %), and variable Zr (43–60 ppm; average 52 ppm), Sr (27–490 ppm; average ~95 ppm) and Ba (4–28 ppm; average 10·3 ppm) contents (Tables 1 and 2). The immobile element contents of the basalts, when plotted on a variety of discriminant diagrams, show MORB-like tectonic affinities with possible arc influence signatures (D'Antonio *et al.*, 2001; Savov *et al.*, 2001; Salisbury *et al.*, 2002). On a total alkalis vs silica (TAS) discriminant diagram (Le Bas *et al.*, 1986) (Fig. 3), almost all of the basement rocks have basaltic compositions. Whereas most of these basalts are subalkaline tholeiites, all of the more evolved lavas are alkalic.

As noted by Savov *et al.* (2001), an N-MORB-like character of the West Philippine basement basalts is revealed by their REE abundances: 1–10 times CI chondrites (CI) in the light REE (LREE; La to Eu) and 10–20 times CI in the middle REE (MREE) and heavy REE (HREE; Eu to Lu) (Fig. 4b; see also Table 7). The chondrite-normalized REE patterns are LREE depleted (mean $[La/Sm]_N = 0{\cdot}49$) but flat in the MREE and HREE (mean $[Gd/Yb]_N = 1{\cdot}00$), which is typical for N-MORB. LREE depletions are variable—from $[La/Sm]_N = 0{\cdot}36$ to $[La/Sm]_N = 0{\cdot}65$–1. One sample (49R-3-37-39) has a similar overall REE pattern to the other samples, but REE abundances are lower by a factor of two than other samples.

Downloaded from http://petrology.oxfordjournals.org/ at Kainan University on March 28, 2015

Table 2: ICP-MS trace element data for selected basement basalts from ODP Site 1201D

Core & section:	46R-1-A	46R-1-B	46R-3	46R-5	47R-3	48R-2	48R-3	48R-4	49R-1	49R-1	49R-3	51R-1	52R-2-A	52R-2-B	53R-1	55R-1
cm interval:	(117–119)	(117–119)	(43–45)	(6–8)	(128–130)	(92–94)	(79–81)	(66–68)	(11–13)	(47–49)	(37–39)	(2–4)	(56–58)	(56–58)	(119–121)	(47–49)
LOI	4·83	4·83	6·55	6·33	—	1·16	1·28	1·26	0·77	1·89	1·52	1·54	1·34	—	1·99	1·49
Li	18·3	17·9	18·3	22·1	13·6	11·6	14·2	13·0	19·5	15·0	3·3	13·8	26·1	26·6	21·0	27·0
Be	0·26	0·25	0·30	0·29	0·25	0·26	0·27	0·22	0·30	0·28	0·11	0·24	0·25	0·25	0·28	0·25
Sc	39·2	42·1	43·3	44·2	39·9	43·1	40·7	42·5	41·24	40·41	42·67	40·30	38·49	41·07	42·86	41·88
TiO_2	0·78	0·79	0·86	0·86	0·82	0·87	0·86	0·86	0·83	0·85	0·87	0·84	0·79	0·81	0·88	0·81
V	229·9	233·0	234·2	238·0	230·0	248·0	244·4	249·1	227·4	242·2	249·7	236·1	236·3	241·7	277·3	247·4
Cr	329·6	332·8	367·9	364·8	396·7	401·3	405·7	402·4	323·3	392·6	398·8	408·2	384·1	385·5	410·2	413·9
Co	35·1	34·9	37·2	39·0	42·9	48·2	47·9	45·4	36·9	49·9	45·2	41·9	42·1	42·5	44·0	45·5
Ni	91·2	86·5	86·6	89·0	121·0	120·5	166·3	129·4	79·8	158·7	106·1	105·3	95·0	95·6	80·3	131·8
Cu	54·7	54·6	79·0	78·7	74·3	148·5	102·2	119·4	73·3	77·9	112·8	52·8	47·1	48·2	63·4	44·4
Zn	58·1	60·1	68·6	68·7	63·1	63·5	62·8	63·4	62·4	61·9	67·0	67·5	66·0	68·7	75·0	58·5
Ga	8·21	8·05	7·00	7·77	8·70	8·54	8·81	8·40	9·44	8·79	8·89	8·86	8·85	8·35	9·36	8·28
As	1·05	0·94	1·61	1·59	0·59	0·79	1·31	0·58	0·93	0·88	0·26	1·04	1·57	1·72	3·64	0·60
Rb	13·14	14·61	14·96	18·30	5·31	6·72	2·34	3·57	18·08	6·76	0·24	5·13	3·54	4·27	5·71	2·59
Sr	273·8	256·2	490·2	322·8	71·5	78·2	81·4	76·4	95·2	78·8	77·8	70·1	83·1	73·5	72·1	79·2
Y	22·2	21·2	27·5	23·7	21·0	23·0	25·6	23·5	23·1	23·1	24·3	20·6	25·5	21·8	22·0	25·0
Zr	54·0	54·0	60·0	58·0	41·0	48·0	49·0	46·9	51·9	50·0	48·2	40·2	52·4	43·3	44·6	—
Nb	1·92	1·26	2·02	1·51	0·73	0·56	0·74	0·50	1·34	0·78	0·46	0·82	0·68	0·52	0·80	0·69
Cs	0·30	0·33	0·35	0·43	0·07	0·13	0·05	0·05	0·46	0·13	—	0·11	0·08	0·09	0·08	0·10
Ba	16·19	16·83	24·31	27·75	5·53	4·45	4·75	4·45	16·46	4·35	6·85	9·09	8·15	9·41	6·09	4·73
La	1·81	1·95	3·23	2·81	1·18	1·33	1·18	1·30	2·44	1·18	0·64	1·26	1·06	1·29	1·23	1·05
Ce	5·53	5·82	6·54	7·14	4·34	4·92	4·28	4·76	6·66	4·38	2·07	4·63	3·99	4·74	4·55	3·97
Pr	0·99	1·03	1·16	1·23	0·86	0·96	0·86	0·93	1·16	0·86	0·42	0·91	0·79	0·92	0·90	0·79
Nd	5·31	5·44	6·00	6·31	4·99	5·53	4·98	5·31	6·03	5·04	2·50	5·22	4·57	5·20	5·25	4·67
Sm	1·90	1·90	2·03	2·21	1·97	2·12	1·95	2·05	2·12	1·98	1·12	2·04	1·82	2·00	2·06	1·88
Eu	0·73	0·71	0·75	0·78	0·76	0·81	0·75	0·78	0·80	0·76	0·51	0·78	0·70	0·77	0·80	0·73
Gd	2·92	2·79	3·17	3·16	3·16	3·23	3·13	3·10	3·08	3·16	1·90	3·23	2·89	3·03	3·23	2·98
Tb	0·55	0·52	0·60	0·60	0·60	0·61	0·59	0·60	0·58	0·60	0·37	0·61	0·54	0·58	0·62	0·57
Dy	3·56	3·43	3·96	3·87	3·91	4·01	3·89	3·87	3·77	3·95	2·53	3·97	3·59	3·76	4·05	3·75
Ho	0·80	0·76	0·91	0·87	0·89	0·89	0·89	0·86	0·85	0·89	0·58	0·91	0·81	0·84	0·93	0·85
Er	2·28	2·15	2·64	2·52	2·51	2·54	2·51	2·47	2·43	2·53	1·66	2·55	2·31	2·40	2·60	2·40
Yb	2·31	2·19	2·72	2·58	2·50	2·55	2·49	2·47	2·48	2·54	1·68	2·54	2·29	2·41	2·61	2·40
Lu	0·36	0·33	0·44	0·40	0·39	0·39	0·39	0·38	0·39	0·39	0·26	0·39	0·36	0·36	0·40	0·37
Hf	—	—	—	2·26	1·41	—	—	1·39	1·45	—	0·62	1·43	1·33	1·33	1·49	—
Ta	0·121	0·109	0·134	0·127	0·066	0·064	0·067	0·060	0·122	0·066	0·048	0·069	0·064	0·059	0·070	0·063
Pb	0·339	0·342	0·560	0·490	0·434	0·246	0·257	0·716	0·406	0·354	2·958	0·313	0·307	0·323	0·253	0·262
Th	0·127	0·119	0·139	0·137	0·044	0·046	0·045	0·044	0·132	0·045	0·029	0·045	0·044	0·045	0·046	0·042
U	0·132	0·123	0·201	0·177	0·158	0·139	0·034	0·154	0·195	0·043	0·008	0·224	0·077	0·081	0·079	0·011

Downloaded from http://petrology.oxfordjournals.org/ at Kainan University on March 28, 2015

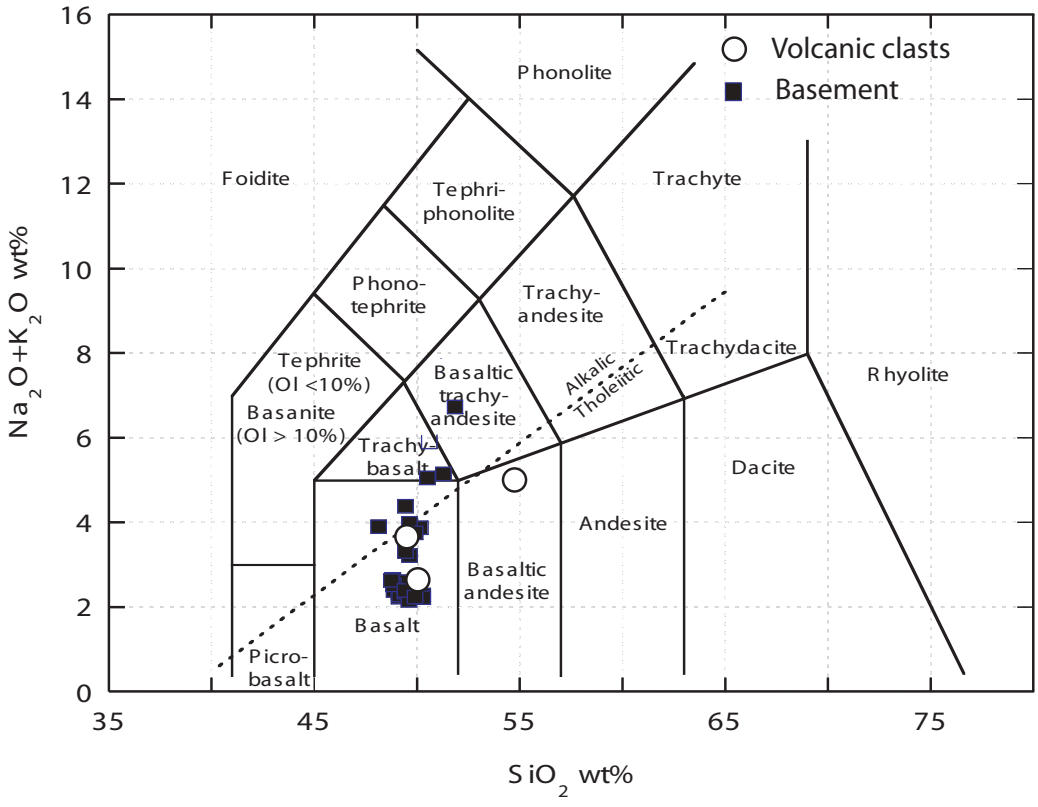

Fig. 3. Total alkali vs silica (TAS) discrimination diagram, showing samples from Site 1201D basement and the volcaniclastic section. After Le Bas *et al.* (1986).

The Site 1201 basement basalts analyzed for trace elements by ICP-MS (Table 2) display some characteristics similar to those of back-arc basin basalts (BABB) on N-MORB-normalized trace element variation diagrams (Fig. 5b). Site 1201D basement basalts have large ion lithophile elements (LILE) Ba, Rb and Cs that are enriched relative to REE and high field strength elements (HFSE), whereas Th is not. They also differ from N-MORB in having average Ba/Th = 149 and Ba/La = 6·4, compared with an average Ba/Th = 60 and Ba/La = 2·5 for N-MORB (see Table 7). Sr and Ba are strongly and variably enriched (256–490 ppm and 16–28 ppm, respectively) in altered basalts from the upper part of the unit, possibly as the result of zeolitization. However, samples from this same upper part of the basement section also have higher abundances of immobile elements LREE, Nb, Ta and Th. Basalts from the upper unit have $[La/Sm]_N$ = 0·6–1·0 and Th/La = 0·043–0·07. All basalts from the lower unit (cores 47–55), except sample 1201D-49R-1 (11–13), have much lower $[La/Sm]_N$ = 0·35–0·40 and Th/La = 0·035–0·041. Sample 1201D-49R-1 (11–13) has immobile trace element abundances like basalts from the upper 20 m of basement basalts ($[La/Sm]_N$ = 0·73 and Th/La = 0·054), but it lacks the strong Sr enrichment (95 ppm Sr). Therefore, there may be primary differences in the trace element patterns of the Site 1201 basement basalts that are partially obscured and overprinted by the effects of seawater alteration.

Normalized trace element patterns of Site 1201D basement basalts in Fig. 5b are similar to that of fresh basaltic glass recovered from West Philippine Basin DSDP Site 447 (Fig. 1) (Hickey-Vargas, 1998*b*), although Ba and, especially, Rb and Cs are more enriched.

Volcaniclastic section

The Palau–Kyushu volcanic clasts selected for geochemical analysis are all basalts with the exception of sample 1201D-10R-4 (63–65), which is an andesite (56 wt % SiO_2; 4·89 wt % $Na_2O + K_2O$; Table 3). Basalt sample 1201D-5R-4 (136-138) is primitive, with 8·1 wt % MgO. LOI values range from 0·8 to 1·7%. All three samples are LREE enriched (Fig. 4a) with LREE 30–50 times CI, and $[La/Sm]_N$ = 2·1–2·8 and HREE 20 times CI, with $[Gd/Yb]_N$ = 1·4–1·7. Andesite 1201D-10R-4 (63–65) has higher REE abundances, but lower La/Sm than the basalts. The Palau–Kyushu rocks have MORB-normalized trace element patterns similar to those of Mariana island arc volcanics (Arculus *et al.*, 1995; Elliott *et al.*, 1997) (Fig. 5a)—high LILE and Th abundances, and

Downloaded from http://petrology.oxfordjournals.org/ at Kainan University on March 28, 2015

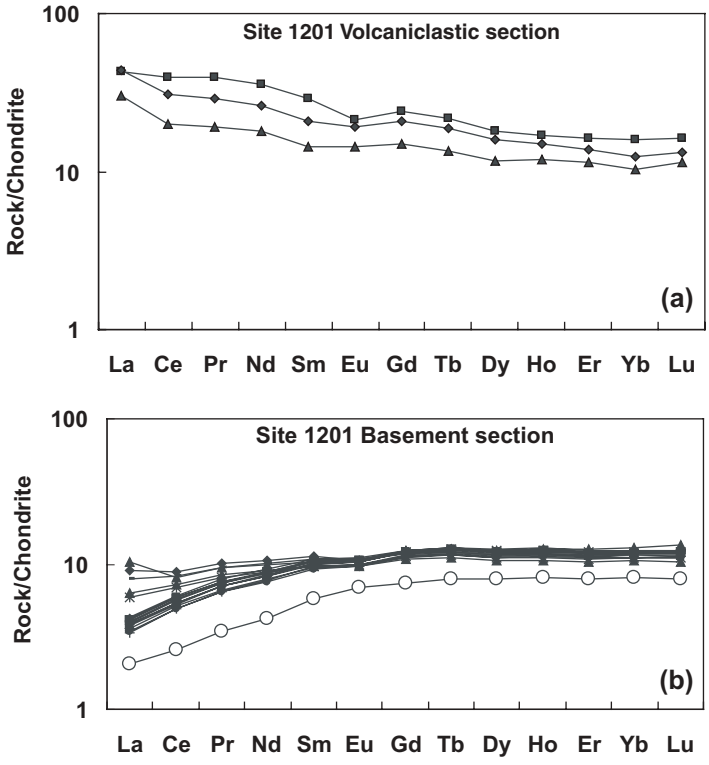

Fig. 4. Chondrite-normalized rare earth element abundances in: (a) clasts from the Site 1201D volcaniclastic section, and (b) the basaltic basement. The typical island arc patterns in the PKR volcaniclasts and the MORB-like patterns of the WPB basement basalts should be noted. All samples are normalized to chondrite values of Nakamura (1974).

large negative Nb and Ta anomalies. The two basalts also show depletion in the HFSE Hf and Zr, whereas the andesite does not. The trace element pattern of the basalts is similar to that in the chemical end-member of the spectrum of basalts erupted in the active Mariana Island arc, which is dominated by a subducted sediment contribution (Fig. 5a, Agrigan; Elliott *et al.*, 1997)).

On a plot of Ba/Th vs $[La/Sm]_N$ (Fig. 6a), the volcanic clasts have higher $[La/Sm]_N$ than the underlying basement basalts but overlapping Ba/Th. Compared with early IBM arc volcanics from other locations (Gill *et al.*, 1994; Hawkins & Castillo, 1998; Pearce *et al.*, 1999) Site 1201D arc volcaniclasts show elevated $[La/Sm]_N$ and similar Ba/Th ratios. When compared with modern Izu and Mariana arc products (Elliott *et al.*, 1997, and references therein), the same rocks show elevated $[La/Sm]_N$ and significantly lower Ba/Th. On a plot of Yb vs TiO_2 (Fig. 6b), the Site 1201D volcanic clasts overlap with Mid-Eocene to Early Miocene volcanic clasts recovered from the Belau islands and the Palau Trench (Hawkins & Castillo, 1998), as well as with 32–36 Ma basalts from Palau–Kyushu Ridge (DSDP Site 448) and the Mariana forearc region (Guam and Saipan) (Taylor, 1992; Gill *et al.*, 1994; Pearce *et al.*, 1999). Their TiO_2 content is lower when compared with the Site 1201D basement basalts and is similar to the TiO_2 contents of both the IBM proto-arc (Pearce *et al.*, 1999) and the modern IBM island arc (Straub, 1997). The opposite is true for the Yb abundances of the studied Site 1201D volcanic clasts. They are similar to the basement basalts but lower than the modern IBM arc (Straub, 1997) and higher than the IBM proto-arc (Pearce *et al.*, 1999).

Isotopes

Basement section

All nine Site 1201D basement basalts analyzed for isotopes were from the lower basement unit (Cores 47–55), which lacks Sr enrichment and has low LOI. Sample 1201D-49R-1 (11–13), which has immobile trace element abundances similar to the altered, upper core section (e.g. higher $[La/Sm]_N$) is included (Tables 2, 4 and 5). Site 1201D West Philippine Basin basalts have initial $^{87}Sr/^{86}Sr$ of 0·70293–0·70320 and $^{143}Nd/^{144}Nd$ of 0·51306–0·51308 (Table 4). On a Sr–Nd isotope co-variation diagram (Fig. 7), all the samples lie within the field of Indian MORB. The basalts are all displaced toward the high-$^{87}Sr/^{86}Sr$ side of the MORB field and toward higher $^{87}Sr/^{86}Sr$ than West Philippine Basin basement basaltic glasses from DSDP Site 447, at a

Downloaded from http://petrology.oxfordjournals.org/ at Kainan University on March 28, 2015

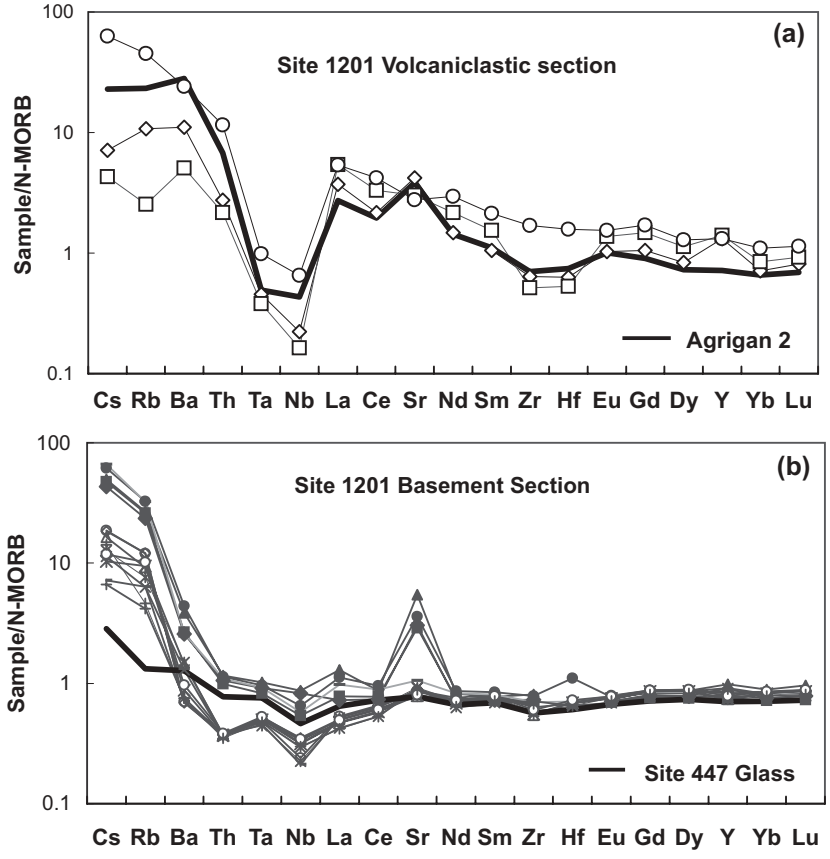

Fig. 5. N-MORB normalized trace element patterns for samples from Site 1201D. Normalizing values are from Sun & McDonough (1989). (a) Volcanic clasts; (b) basement basalts. In (a) volcanic clasts are compared with a basalt from the current Mariana island arc volcanic front (Agrigan-2) (Elliott *et al.*, 1997). In (b) basement basalts are compared with a basaltic glass from DSDP Site 447 (Hickey-Vargas, 1998*b*), which is near Site 1201D.

nearly constant $^{143}Nd/^{144}Nd$ value. There is no systematic Sr- and Nd-isotopic difference between basalts with high and low $[La/Sm]_N$ (Table 4).

The basement basalts span a narrow range of initial Pb isotope ratios: 17·78–18·19 ($^{206}Pb/^{204}Pb$), 15·45–15·52 ($^{207}Pb/^{204}Pb$) and 37·69–37·96 ($^{208}Pb/^{204}Pb$) (Table 5; Fig. 8). These values are similar to those of basalts recovered from DSDP Site 447 in the West Philippine Basin to the SW (Hickey-Vargas, 1991, 1998*a*). Most of the Site 1201D basement basalts have higher $^{208}Pb/^{204}Pb$ for a given $^{206}Pb/^{204}Pb$ compared with Pacific MORB; this is a characteristic of other West Philippine Basin basement basalts (Hickey-Vargas, 1991, 1998*a*, 1998*b*; Hickey-Vargas *et al.*, 1995), i.e. they are more similar to Indian Ocean MORB. However, two samples, 1201D-51R-1 (2–4) and 1201D-49R-3 (37–39), are slightly shifted toward higher $^{206}Pb/^{204}Pb$ and approach the Pacific MORB field (Fig. 8). There is no systematic difference in Pb-isotopes between basalts with high and low $[La/Sm]_N$ (Table 5).

Recent results (Pearce *et al.*, 1999; Hickey-Vargas *et al.*, 2005) have shown that West Philippine Basin basalts also exhibit an Indian MORB Nd–Hf isotope signature, marked by a higher $^{176}Hf/^{177}Hf$ for a given $^{143}Nd/^{144}Nd$ compared with Pacific MORB. Three Site 1201D basement basalts plot in a cluster (initial $^{176}Hf/^{177}Hf = 0{\cdot}28327–0{\cdot}28330$, Fig. 9c) near a value reported for DSDP Site 447 (Pearce *et al.*, 1999; Hickey-Vargas *et al.*, 2005). Although two of these three samples are shifted toward the Pacific MORB field on the Pb–Pb plot (Fig. 8), such a spread is not shown by Hf vs Nd isotopes.

Volcaniclastic section

The three Palau–Kyushu arc-derived clasts have higher and more variable initial Sr isotope ratios (0·70338–0·70432, Table 4, Fig. 7), than the basement basalts. The clasts also have slightly more radiogenic Pb-isotope ratios, 18·37–18·41 ($^{206}Pb/^{204}Pb$), 15·51–15·52 ($^{207}Pb/^{204}Pb$) and 38·18–38·23 ($^{208}Pb/^{204}Pb$) (Table 5, Fig. 8). These values are within the broad range defined by other southern Palau–Kyushu arc samples from Guam, Saipan, DSDP Sites 448, 458 and 459, as well as dredge samples from the Mariana Trench (Hickey-Vargas &

Downloaded from http://petrology.oxfordjournals.org/ at Kainan University on March 28, 2015

Table 3: Major and trace elements in volcanic clasts from Site 1201D

Core & section:	5R4	5R4	10R4
cm interval:	(110–112)	(136–138)	(63–65)
Depth (mbsf):	123·98	124·24	171·92
SiO_2	48·90	50·35	54·75
TiO_2	0·57	0·43	0·74
Al_2O_3	20·81	17·37	19·05
Fe_2O_3	7·84	9·18	8·52
MnO	0·15	0·16	0·15
MgO	4·22	8·10	4·09
CaO	11·98	11·51	7·16
Na_2O	3·16	2·33	3·95
K_2O	0·66	0·22	1·16
P_2O_5	0·23	0·20	0·41
Total	98·52	99·85	99·98
LOI	1·66	1·40	0·81
Li	8·76	10·07	9·66
Be	0·73	0·54	1·09
Sc	27·6	37·3	26·1
TiO_2	0·57	0·43	0·74
V	264	219	176
Cr	12·9	139·3	10·3
Co	21·6	32·5	21·6
Ni	13·2	49·0	21·8
Cu	58·4	58·1	37·7
Zn	79·2	68·6	94·9
Ga	15·8	12·9	23·8
As	0·29	0·34	1·11
Rb	6·04	1·42	25·29
Sr	378·5	272·4	249·6
Y	36·8	39·3	36·9
Zr	47·4	38·2	125·4
Nb	0·52	0·38	1·52
Cs	0·05	0·03	0·44
Ba	69·7	31·9	152·3
La	9·3	13·5	13·4
Ce	16·2	24·9	31·6
Pr	2·33	3·51	4·85
Nd	10·8	15·8	21·5
Sm	2·77	4·06	5·62
Eu	1·05	1·40	1·57
Gd	3·88	5·43	6·29
Tb	0·63	0·89	1·02
Dy	3·79	5·13	5·86
Ho	0·86	1·08	1·21
Er	2·42	2·89	3·41
Yb	2·17	2·58	3·36
Lu	0·37	0·42	0·52
Hf	1·29	1·09	3·24
Ta	0·06	0·05	0·13
Pb	1·81	2·30	3·49
Th	0·33	0·26	1·38
U	3·79	0·74	0·63

Reagan, 1987; Hickey-Vargas, 1989, 1991; Stern *et al.*, 1991; Pearce *et al.*, 1999; Reagan *et al.*, 2002). Like the basement basalts, Site 1201D clasts plot within the Indian MORB field on a plot of $^{176}Hf/^{177}Hf$ vs $^{143}Nd/^{144}Nd$ (Fig. 9c), at slightly lower initial $^{143}Nd/^{144}Nd$ (0·51297–0·51298) and initial $^{176}Hf/^{177}Hf$ (0·28321–0·28326) values than the basement basalts (Table 6, Fig. 9c).

DISCUSSION

Origin of basement basalts

Two models have been proposed to explain the origin of the West Philippine Basin in the context of the evolving intra-oceanic Izu–Bonin–Mariana convergent margin. The first model proposes that the West Philippine Basin is a large piece of trapped spreading ridge of the North New Guinea–Pacific oceanic crust, based on magnetic anomaly data and the observed high angle between the fossil spreading axis (Central Basin Fault) and the paleo-volcanic arc (Palau–Kyushu Ridge) (Hilde & Lee, 1984). The second model describes the West Philippine Basin as a back-arc basin, which opened between two active subduction zones and was progressively rotated clockwise (Hall *et al.*, 1995; Deschamps & Lallemand, 2002; Reagan *et al.*, 2002). These models can be tested by examining West Philippine Basin basalts for MORB vs BABB character.

Rocks previously recovered from the West Philippine Basin floor during DSDP Legs 58 and 59 have a wide range of chemical affinities from N-MORB-like to OIB-like (Figs 6–8; Mattey *et al.*, 1981; Hickey-Vargas, 1991, 1998*a*, 1998*b*). Rocks recovered from Site 1201D fall at the MORB-like end of this range, both in their trace element and Sr–Nd–Pb–Hf isotopic characteristics (Figs 4–9). Like all other West Philippine Basin MORB and OIB-like basalts studied to date, the Sr–Nd–Pb–Hf isotopic characteristics of the Site 1201D basement basalts show largely Indian Ocean MORB-like isotopic signatures, suggesting that Philippine Sea Plate magmatism tapped an upper mantle domain that was distinct from that underlying the Pacific spreading ridges and islands.

Compared with MORB worldwide and N-MORB-like West Philippine Basin basalts from DSDP Site 447, all Site 1201D basement basalts are strongly enriched in Cs and Rb, and those from the upper section have high Ba and Sr (Fig. 5). $^{87}Sr/^{86}Sr$ isotopic ratios in basalts from the lower section are slightly higher than those from DSDP Site 447, but $^{143}Nd/^{144}Nd$, $^{176}Hf/^{177}Hf$ and Pb-isotopic ratios are similar. Our interpretation is that the elevated $^{87}Sr/^{86}Sr$, and Cs and Rb enrichment are probably related to pervasive seawater alteration. This is supported in part by the fact that the analyzed Site 447 samples are hand-picked glasses (Hickey-Vargas, 1991,

Downloaded from http://petrology.oxfordjournals.org/ at Kainan University on March 28, 2015

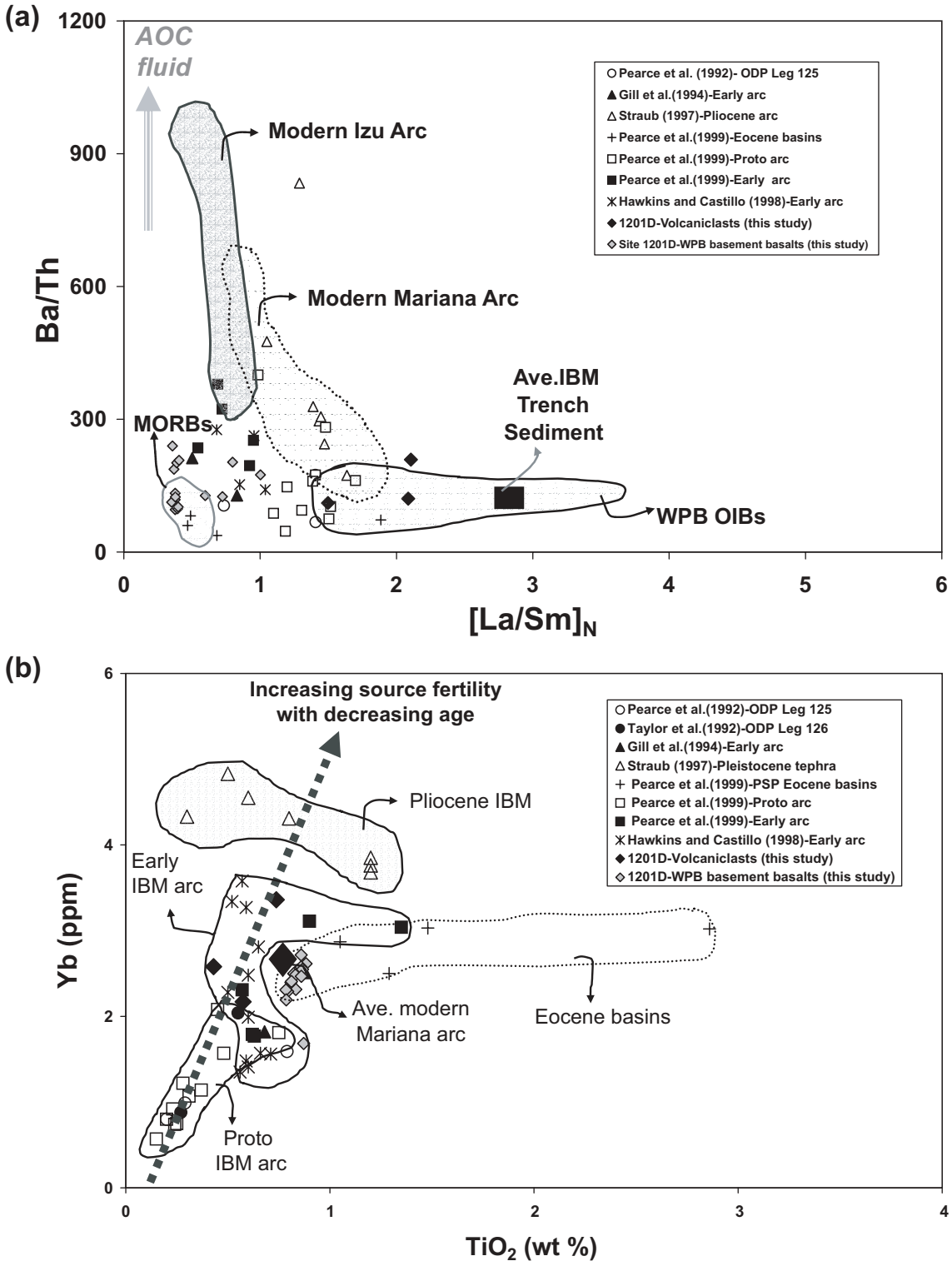

Fig. 6. Plots of $[La/Sm]_N$ vs Ba/Th (a) and TiO_2 vs Yb (b) for ODP Site 1201D arc volcaniclasts and WPB basement basalts. For comparison are also shown other early IBM arc volcanics from the literature (Gill *et al.*, 1994; Hawkins & Castillo, 1998; Pearce *et al.*, 1999), Eocene Basins on the Philippine Sea Plate (PSP) (Pearce *et al.*, 1999), as well as modern Izu and Mariana arc products (Elliott *et al.*, 1997; Straub, 1997). AOC, altered oceanic crust; AOC-fluid and MORB (mid-ocean ridge basalt) fields are after Elliott (2003). The reported $[La/Sm]_N$ ratios were normalized to chondrite meteorite values reported by Nakamura (1974). The decreasing effect of sediment additions and the increasing degree of mantle source fertility occurring during the transition from proto-IBM to Pliocene IBM arc products should be noted.

Downloaded from http://petrology.oxfordjournals.org/ at Kainan University on March 28, 2015

Table 4: Sr and Nd isotope data for selected samples from ODP Site 1201D

Sample	$^{87}Sr/^{86}Sr_{meas.}$	2σ*	Rb/Sr	$^{87}Sr/^{86}Sr_{init.}$†	$^{143}Nd/^{144}Nd_{meas.}$	2σ	Sm/Nd	$^{143}Nd/^{144}Nd_{init.}$	$\varepsilon_{Nd}(t)$‡
Volcaniclastic section (35 Ma)									
195-1201D-5R-4 (110–112)	0·704341	0·000008	0·016	0·704318	0·513007	0·000005	0·258	0·512971	7·35
195-1201D-5R-4 (136–138)	0·70394	0·000009	0·005	0·703933	0·513002	0·000006	0·257	0·512967	7·25
195-1201D-10R-4 (63–66)	0·703523	0·000008	0·101	0·703377	0·513013	0·000006	0·261	0·512977	7·45
Basement section (45 Ma)									
195-1201D-48R-2 (92–94)	0·703103	0·000009	0·086	0·702944	0·513134	0·000004	0·383	0·513066	9·44
195-1201D-48R-4 (66–68)	0·703016	0·000008	0·047	0·702930	0·513143	0·000004	0·386	0·513075	9·61
195-1201D-49R-1 (11–14)	0·703026	0·000007	0·042	0·702949	0·513148	0·000005	0·392	0·513078	9·68
195-1201D-49R-1 (47–49)	0·703186	0·000006	0·086	0·703027	0·513139	0·000003	0·393	0·513069	9·51
195-1201D-49R-3 (37–39)	0·703202	0·000008	0·003	0·703196	0·513135	0·000006	0·448	0·513056	9·24
195–1201D-51R-1 (2–4)	0·703147	0·000007	0·073	0·703012	0·513136	0·000004	0·391	0·513067	9·46
195-1201D-52R-2 (56–58)	0·703153	0·000007	0·050	0·703061	0·513142	0·000006	0·391	0·513073	9·57
195-1201D-53R-1 (119–121)	0·703193	0·000007	0·079	0·703047	0·513139	0·000004	0·392	0·513069	9·51
195-1201D-55R-1 (47–49)	0·703034	0·000006	0·033	0·702974	0·513141	0·000004	0·403	0·513070	9·51

*Two sigma of the mean.
†Initial ratios for the volcaniclastic section are calculated to 35 Ma; initial ratios for the basement section are corrected to 45 Ma.
‡$\varepsilon_{Nd}(t)$ is calculated using present-day values $^{143}Nd/^{144}Nd = 0{\cdot}51264$ and $^{147}Sm/^{144}Nd = 0{\cdot}1967$ for CHUR.

Table 5: Pb isotope ratios for samples from ODP Site 1201D

Sample	$^{206}Pb/^{204}Pb_{meas.}$*	$^{207}Pb/^{204}Pb_{meas.}$	$^{208}Pb/^{204}Pb_{meas.}$	U/Pb	Th/Pb	$^{206}Pb/^{204}Pb_{init.}$†	$^{207}Pb/^{204}Pb_{init.}$	$^{208}Pb/^{204}Pb_{init.}$
Volcaniclastic section (35 Ma)								
195-1201D-5R-4 (110–112)	19·100	15·555	38·255	2·094	0·182	18·372	15·521	38·234
(duplicate)	19·099	15·550	38·230	2·094	0·182	18·372	15·516	38·209
195-1201D-5R-4 (136–138)	18·521	15·519	38·225	0·322	0·113	18·410	15·514	38·212
195-1201D-10R-4 (63–66)	18·468	15·519	38·221	0·181	0·395	18·406	15·516	38·176
Basement section (45 Ma)								
195-1201D-48R-2 (92–94)	18·181	15·480	37·840	0·565	0·187	17·933	15·468	37·813
195-1201D-48R-4 (66–68)	17·870	15·524	37·703	0·215	0·061	17·776	15·520	37·694
195-1201D-49R-1 (11–14)	18·092	15·461	37·780	0·480	0·325	17·882	15·451	37·733
195-1201D-49R-1 (47–49)	18·121	15·505	37·976	0·121	0·127	18·068	15·502	37·958
195-1201D-49R-3 (37–39)	18·189	15·481	37·823	0·003	0·010	18·188	15·481	37·822
195-1201D-51R-1 (2–4)	18·482	15·519	37·971	0·716	0·144	18·166	15·504	37·950
195-1201D-52R-2 (56–58)	18·001	15·496	37·769	0·251	0·143	17·892	15·491	37·748
195-1201D-53R-1 (119–121)	18·168	15·489	37·901	0·312	0·182	18·031	15·483	37·875
(duplicate)	18·157	15·476	37·862	0·312	0·182	18·020	15·469	37·835
195-1201D-55R-1 (47–49)	18·017	15·454	37·773	0·042	0·160	17·999	15·453	37·750
(duplicate)	18·013	15·450	37·757	0·042	0·160	17·995	15·449	37·733

*Typical external reproducibility is ±0·05% per a.m.u.
†Initial ratios for the volcaniclastic section are corrected to 35 Ma; initial ratios for the basement section are corrected to 45 Ma.

Downloaded from http://petrology.oxfordjournals.org/ at Kainan University on March 28, 2015

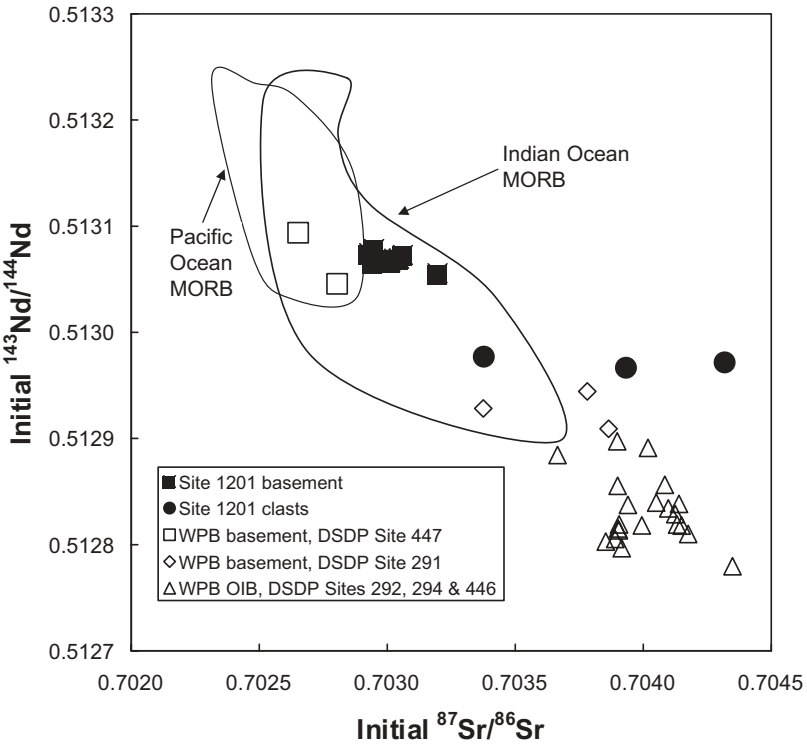

Fig. 7. Initial $^{87}Sr/^{86}Sr$ vs initial $^{143}Nd/^{144}Nd$ for samples from ODP Site 1201D, compared with fields for Pacific and Indian MORB, MORB-like and OIB-like basalts from the West Philippine Basin. Data for West Philippine Basin basalts are from Hickey-Vargas (1991, 1998*b*). MORB data are from sources listed by Hickey-Vargas (1998*b*). Analytical errors (Table 4) are smaller than the symbols plotted.

1998*a*), whereas Site 1201D samples are holocrystalline, and that zeolites are observed in the upper Site 1201D unit (D'Antonio & Kristensen, 2004). An N-MORB character for the Site 1201D basalts is also supported by the extremely low $[La/Sm]_N$ and Th/La ratios found in the lower section (Table 7). However, because Ba, Sr, Cs and Rb are all mobile elements, it is difficult to distinguish post-eruptive alteration from addition of hydrous subduction fluids to the source of the basalts, as is observed in some BABB (e.g. Stolper & Newman, 1994).

An alternate source of enrichment, mantle source enrichment by OIB-like melts or veins, which is a proposed origin for E-MORB (e.g. Wood, 1979), including E-MORB from DSDP Site 291 (Hickey-Vargas *et al.*, 2005), is also not consistent with the pattern of trace element enrichment in the Site 1201D basement section. Because there is no isotopic difference between samples with relatively higher and lower Th, Nb, Ta and LREE, it is likely that these differences are related to sub-ridge partial melting processes (e.g. Langmuir *et al.*, 1992).

Sources for early Izu–Bonin–Mariana basaltic magmas

Site 1201D is the only location among older IBM arc locales where a volcaniclastic section containing early-IBM arc basalts is found directly overlying West Philippine Basin basalts. This provides a near-ideal situation in which to examine the relative importance of subduction materials and processes vs pre-subduction mantle wedge heterogeneity in producing the geochemical characteristics of the early IBM arc basalts.

Although the exact nature of the sediment column subducted beneath the early IBM arc cannot be reconstructed, specific sediment types subducting beneath the active IBM arc can be used to define the range of possible compositions. As this sediment column is largely Cretaceous in age (Elliott *et al.*, 1997; Plank & Langmuir, 1998), it pre-dates the initiation of subduction and the eruption clasts within the Site 1201D volcaniclastic section. Pacific sediment end-members defined by Elliott *et al.* (1997) are: pelagic clays (CL), cherts (CH) and seamount-derived volcaniclastics (V). Based on the occurrence of OIB-like basalts in the West Philippine Basin, Macpherson & Hall (2001) and Deschamps & Lallemand (2005) hypothesized that a hotspot located in the West Philippine Basin could have provided the anomalous heat required for the production of voluminous boninites in the early proto-IBM arc. Although the only evidence for eruption of voluminous OIB is the Benham Rise, in the far western West Philippine Basin, the scattered occurrence of OIB in deep areas of the basin such as DSDP

Downloaded from http://petrology.oxfordjournals.org/ at Kainan University on March 28, 2015

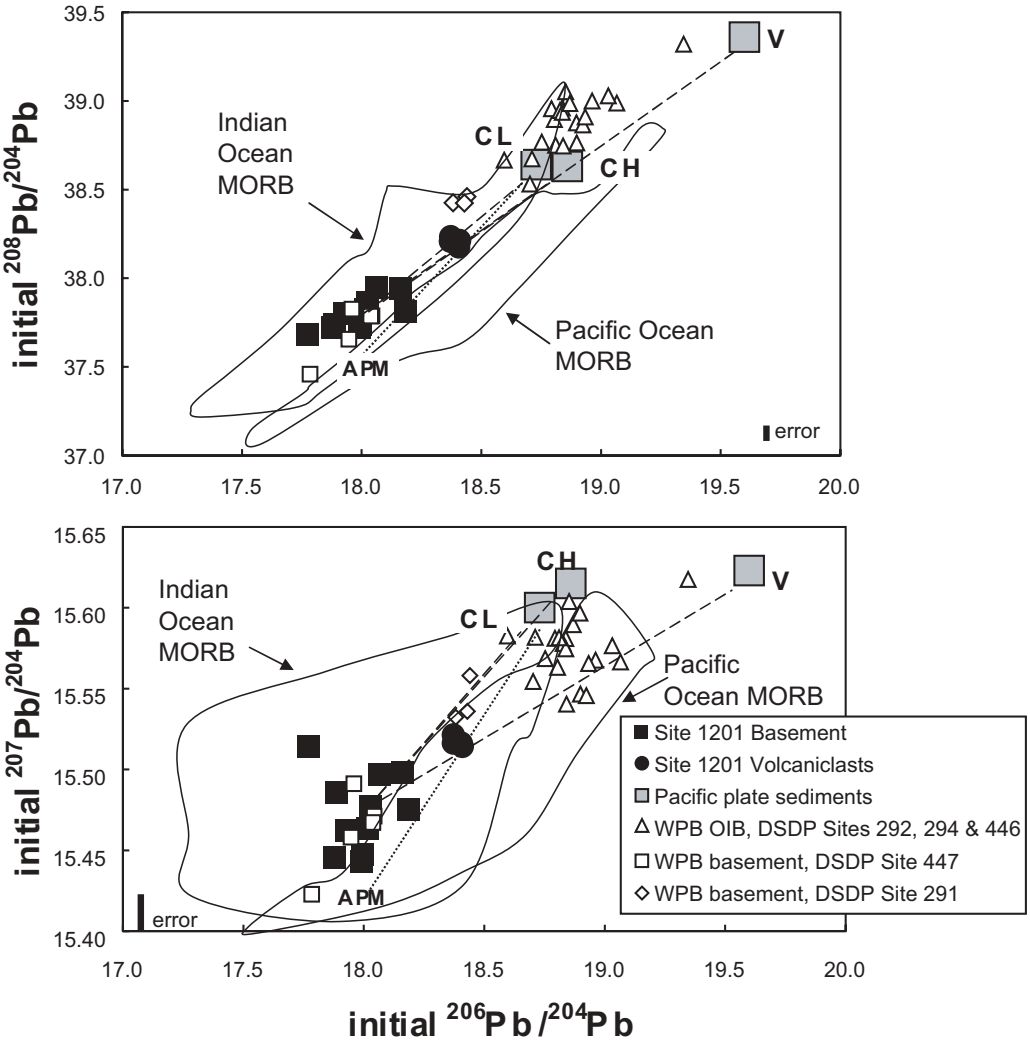

Fig. 8. Initial $^{208}Pb/^{204}Pb$ and $^{207}Pb/^{204}Pb$ vs $^{206}Pb/^{204}Pb$ in basement basalts and volcanic clasts from ODP Site 1201D. Fields for Pacific and Indian Ocean MORB, MORB-like and OIB-like basalts from the WPB (Hickey-Vargas, 1991, 1998*b*), and Pacific Plate sediments (Elliott *et al.*, 1997; Pearce *et al.*, 1999) are shown for comparison. Mixing lines (dashed) are drawn between the mantle source for Site 1201D basement basalts and sediments. Pacific plate sediment types: CL, clay; CH, chert; V, seamount (OIB)-derived volcaniclastic sediment. A dotted mixing line is drawn between clay-rich sediment (CL) and altered Pacific MORB (APM). MORB values are from sources listed by Hickey-Vargas (1998*b*).

Site 294 and 446 suggests that OIB sources may be 'embedded' in the West Philippine Basin upper mantle. For this reason, both subducted sediment and West Philippine Basin OIB mantle sources are considered in the following discussion.

Sr–Nd–Pb–Hf isotope and trace element ratios (Table 7, Figs 6–9) are useful in distinguishing potential source materials. Assuming that the basement basalts can be used to infer the mantle source composition for the subsequent arc basalts, the lower $^{143}Nd/^{144}Nd$ and higher $^{87}Sr/^{86}Sr$ of the arc basalts could result from admixture of a small amount of any of the Pacific sediment types [pelagic clays (CL), cherts (CH) and seamount-derived volcaniclastics (V)], or West Philippine Basin OIB sources, into the sub-arc mantle wedge (Fig. 9a and Table 7). The curvature of mixing lines between mantle and clay-rich and siliceous subducted sediments in Fig. 9a results from the low Sr/Nd for these sediments or sediment melt (Elliott *et al.*, 1997; Table 7). In contrast, like many arc basalts, the Site 1201D volcanic clasts have higher than MORB-like Sr/Nd (Table 7), which requires a source of additional Sr, less radiogenic than subducted sediment. As proposed by many workers [see references given by Elliott (2003)], this source could be a Sr-rich fluid phase expelled from subducted altered Pacific MORB (Fig. 9a). Mixing with West Philippine Basin OIB mantle sources or subducted Pacific OIB-derived volcaniclastic sediments (V) could

Downloaded from http://petrology.oxfordjournals.org/ at Kainan University on March 28, 2015

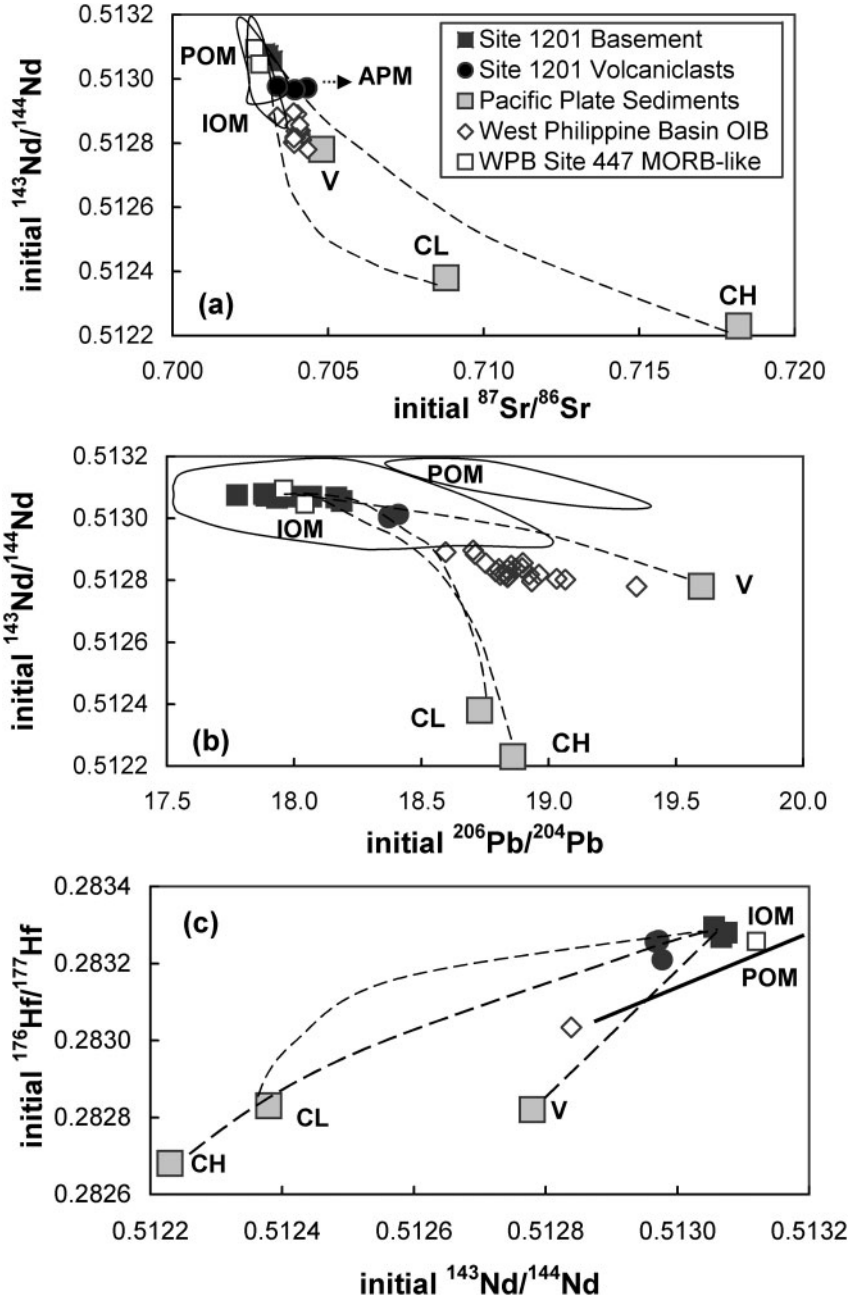

Fig. 9. Nd–Sr–Pb–Hf isotopic ratios in Site 1201D basement basalts and volcanic clasts compared with fields for Pacific Ocean MORB (POM) and Indian Ocean MORB (IOM), West Philippine Basin (WPB) MORB-like and OIB-like basalts (Hickey-Vargas, 1991, 1998*a*, 1998*b*; Pearce *et al.*, 1999) and three types of Pacific plate sediment: (a) $^{143}Nd/^{144}Nd$ vs $^{87}Sr/^{86}Sr$; (b) $^{143}Nd/^{144}Nd$ vs $^{206}Pb/^{204}Pb$; (c) $^{176}Hf/^{177}Hf$ vs $^{143}Nd/^{144}Nd$. Pacific plate sediment types: CL, clay; CH, chert; V, seamount (OIB)-derived volcaniclastic sediment. Trace element ratios are from Elliott *et al.* (1997) and isotopic ratios are calculated from data from Pearce *et al.* (1999). Mixing curves (dashed) are drawn from the mantle source of Site 1201D basement basalts to sediments. APM in (a) stands for altered Pacific MORB. A continuous line in (c) divides the fields for IOM and POM, after Pearce *et al.* (1999). Analytical errors (Tables 4–6) are smaller than the data symbols plotted.

also explain the lower $^{143}Nd/^{144}Nd$ in the arc magmas, but not the elevated Sr/Nd (Table 7).

Based on the Pb-isotope data (Fig. 8), simple mantle–sediment or mantle–West Philippine Basin OIB source mixing can explain the offset between basement and arc basalts. For clay-rich (CL) and siliceous sediments (CH), which have high $^{207}Pb/^{204}Pb$ for a given $^{206}Pb/^{204}Pb$, an end-member with low $^{207}Pb/^{204}Pb$ is suggested, rather than the average composition of the basement basalts. Like nearly all arc basalts, the volcaniclastic samples have

Downloaded from http://petrology.oxfordjournals.org/ at Kainan University on March 28, 2015

Table 6: Hf isotope data for samples from ODP Site 1201D

Sample	$^{176}Hf/^{177}Hf_{meas.}$	2σ of mean	Lu/Hf	$^{176}Hf/^{177}Hf_{init.}$*	$\varepsilon_{Hf}(t)$†
Volcaniclastic section (35 Ma)					
195-1201D-5R-4 (110–112)	0·283287	0·00002	0·287	0·283259	18·04
195-1201D-5R-4 (136–138)	0·283272	0·000017	0·163	0·283256	17·94
195-1201D-10R-4 (63–66)	0·283225	0·000009	0·160	0·283209	16·28
Basement section (45 Ma)					
195-1201D-48R-4 (66–68)	0·283314	0·000022	0·273	0·283280	20·20
195-1201D-49R-3 (37–39)	0·283347	0·000029	0·417	0·283295	21·36
195-1201D-51R-1 (2–4)	0·283302	0·000016	0·273	0·283268	19·77

*Initial ratios for the volcaniclastic section are corrected to 35 Ma, and initial ratios for the basement section are corrected to 45 Ma.
†$\varepsilon_{Hf}(t)$ is calculated using present-day $^{176}Hf/^{177}Hf = 0{\cdot}282772$ and $^{176}Lu/^{177}Hf = 0{\cdot}0332$.

higher Pb/Ce and Pb/Nd than MORB or OIB (Table 7). This observation favors sediment admixture as an explanation, because high Pb/Nd is characteristic of pelagic sediments (Table 7). However, excess Pb could also be carried in a fluid derived from altered subducted MORB (Elliott, 2003). In this latter case, mixing lines through the arc lavas may extend from Pacific sediment to altered Pacific MORB, rather than to the basement basalts (Fig. 8), accounting for the somewhat low $^{207}Pb/^{204}Pb$ inferred for the second mixing end-member.

In Fig. 9b, the curvature of mixing lines between mantle and clay-rich or siliceous sediments through the arc volcanics results from the higher Pb/Nd in the sediments compared with the mantle end-member. In contrast, mixing of mantle with Pacific volcaniclastic sediments, and especially West Philippine Basin OIB-source mantle, is linear, because the two end-members have similar Pb/Nd (Table 7). Thus these materials do not account for the elevated Pb/Nd in the arc volcanics.

Figure 9c shows mixing relationships on a plot of $^{176}Hf/^{177}Hf$ vs $^{143}Nd/^{144}Nd$. The sense of the Nd isotopic shift of the Site 1201D clasts compared with basement is consistent with mixing of mantle with a clay-rich or siliceous sediment or sediment melt with low Hf/Nd, but not with mixing with OIB-derived volcaniclastic sediment. Mixing with West Philippine Basin OIB-sources is also plausible as mixing lines would be linear. However, as shown in Table 7, Hf/Nd in the volcanic clasts is lower than those of the basement basalts, which is a characteristic of clay-rich sediment, but not West Philippine Basin OIB.

In general, therefore, the isotopic shift between Site 1201D basement basalts and the overlying early IBM volcanic clasts is consistent with either addition of a small percentage of subducted clay-rich sediment or incorporation of a small amount of OIB-source mantle. However, trace element constraints favor sediment addition, particularly addition of the clay-rich end-member (CL), because such mixing can also explain the low Hf/Nd ratios and contribute to the high Pb/Nd in the arc volcanics. About 0·1% of the clay-rich end-member added to the mantle source of the basin basalts closely matches the Pb, Hf and Nd isotopic composition of the volcanic clasts, and the $^{87}Sr/^{86}Sr$ isotope ratio of the least radiogenic sample. Based on these observations, we conclude that the most likely explanation for both isotopic and trace element differences between the Site 1201D West Philippine Basin basement basalts and overlying arc-volcanic clasts is that a small amount of subducted sediment or sediment melt was incorporated into melts generated in the mantle wedge (Indian MORB source), together with Sr- and Pb-rich hydrous fluids from subducted Pacfic MORB basalt.

Using the clay-rich sediment end-member (CL), and basement basalt 1201D-55R-1, we estimate that about 15% of the Sr and Nd, about 50% of the Pb and less than 5% of the Hf in the arc basalts are derived from subducted sediment. Recent controversy has centered on whether Hf is mobilized by subduction processes (Pearce *et al.*, 1999; Woodhead *et al.*, 2001; Prinkney *et al.*, 2002). This result suggests that a small amount of Hf can be mobilized, in this case by bulk sediment incorporation or sediment melting.

Implications for a hotspot in the eastern part of the West Philippine Basin

Geochemical arguments mitigate against an OIB mantle source component for both the MORB-like West Philippine Basin basement basalts and the early IBM arc volcanics sampled in the upper section of Site 1201D. Taken together, geochemical and geological evidence suggests that although a mantle hotspot may have formed the Benham Rise in the western West Philippine Basin during the Eocene, its geochemical influence apparently did not extend to the eastern West Philippine Basin near ODP Site 1201D or DSDP Site 447. As these locations are closest to the Palau–Kyushu Ridge near the reconstructed location of the Bonin Islands before opening of the Shikoku Basin (Deschamps & Lallemand, 2005), this observation does not support the hypothesis that a mantle hotspot provided the heat needed to trigger boninitic

Downloaded from http://petrology.oxfordjournals.org/ at Kainan University on March 28, 2015

Table 7: Average trace element ratios in Site 1201D basement basalts, volcaniclastics and possible source materials

	Site 1201D				Site 1201D	Pacific sediments		
	Basement basalts*	Primitive mantle†	Normal MORB†	WPB OIB‡	Arc volcaniclastics§	Clay (CL)	Chert (CH)	Volcanic (V)
Sr/Nd	15·0	15·6	12·3	15·5	20·8	1·6	6·9	12·5
Pb/Nd	0·068	0·052	0·041	0·056	0·159	0·377	0·382	0·130
Hf/Nd	0·263	0·228	0·281	0·157	0·113	0·034	0·127	0·190
$(La/Sm)_n$	0·49	1·00	0·61	2·06	1·95	2·49	2·87	2·98
$(Gd/Yb)_n$	1·00	1·00	1·00	2·55	1·59	1·86	1·59	2·55
La/Nb	1·7	0·96	1·07	0·81	18·8	7·94	1·79	0·80
Ba/La	6·4	10·2	2·52	9·14	7·07	3·07	10·4	6·58
Ba/Th	149	82	53	104	133	33	62	52
Th/La	0·043	0·124	0·048	0·088	0·053	0·092	0·167	0·126

*Average of eight basalts analyzed for isotopes from Table 2.
†From Sun & McDonough (1989).
‡Average of 17 WPB OIB from Hickey-Vargas (1998*b*).
§Average of three samples in Table 3.
From Elliott *et al*. (1997).

volcanism in the early IBM arc (Macpherson & Hall, 2001; Deschamps & Lallemand, 2005).

Temporal changes in the sources of IBM arc magmas

Eocene to Oligocene IBM arc volcanic rock samples are very limited and their recovery locations may not be representative for the entire spread and nature of IBM arc volcanism. Therefore, it is difficult to evaluate the temporal geochemical changes that took place in the mantle source regions as the IBM arc evolved. In Fig. 6a and b, the new Site 1201 samples from both the West Philippine Basin basement and the overlying early arc volcanic sequence are compared with existing West Philippine Basin and early IBM arc datasets (Gill *et al.*, 1994; Straub, 1997; Hawkins & Castillo, 1998; Pearce *et al.*, 1999). In Fig. 6a, the Site 1201 clasts plot at relatively high $[La/Sm]_N$ and low Ba/Th, which indicates dominance of sediment or sediment melt over fluids from the altered oceanic crust (AOC fluids) (Elliott, 2003). This is consistent with our interpretation based on other trace element and isotopic constraints. Based on Fig. 6a, it is apparent that sometime in the late Eocene the erupted island arc volcanic products began to experience less of the effect of the subducted sediments (appearance of volcanic rocks with lower $[La/Sm]_N$). The subduction signal shifted toward AOC fluid-dominated signatures, similar to the one currently present in the modern Izu and Mariana island arc volcanic products (i.e. Elliott, 2003; high Ba/Th and low$[La/Sm]_N$).

Using the immobile elements Yb and TiO_2 as tracers, in Fig. 6b we see an increase in Yb and TiO_2 abundances accompanying the transition between Eocene boninites and island arc tholeiites (proto-IBM arc), and the Site 1201 and other early IBM arc volcanic rocks. As Yb and TiO_2 are not likely to be transported from the subducted slab, this indicates an increase in the fertility of the mantle source regions producing the early IBM arc magmas. The mantle source regions become even more fertile in the Pliocene Izu segment of the island arc [see the tephras of Straub (1997)], which are similar to the average modern Mariana island arc lavas (TiO_2/Yb ~0·34, Elliott *et al.*, 1997).

One possible explanation for both trends is that the early IBM subduction zone was significantly hotter than at present. Models of the initiation of the IBM arc (Stern, 2004) show that the early stage of subduction is accompanied by asthenospheric upwelling over the shallow parts of the downgoing plate. This leads to the generation of boninite by extensive, hydrous, low-pressure melting of the mantle wedge and would also lead to the high temperatures at the slab surface needed to cause melting of sediment on the subducting plate. With gradually maturing subduction, the upper oceanic crust and mantle wedge will cool, allowing hydrous fluids to be subducted into the zone of arc magma generation, resulting in flux melting and the dominance of AOC-fluid vs sediment melt signatures in the young samples. In this scenario, increasing Yb and TiO_2 contents could be linked to decreasing extents of melting to produce arc magma, and increasing source fertility as a result of replenishment

Downloaded from http://petrology.oxfordjournals.org/ at Kainan University on March 28, 2015

of the mantle wedge by convection. The pattern of volcanic sediment accumulation at Site 1201 indicates that maximum delivery of volcanic debris occurred in the late Eocene–early Oligocene (35–30 Ma), toward the end of the activity of the early IBM arc (Cosca *et al.*, 1998), and just prior to the beginning of rifting and opening of the Shikoku Basin at about 28 Ma (Okino *et al.*, 1999). Such a pattern could indicate maximum growth of the northern IBM arc at this time, and possibly maximum rates of magma production, which also supports increasing source fertility. Rigorous evaluation of these trends requires a much larger body of geochemical data and better constraints on the ages of early IBM volcanic rocks than are available at present.

SUMMARY AND CONCLUSIONS

Based on geological, petrological and geochemical information, the basement and overlying volcaniclastic section recovered at ODP Site 1201D represents the pre-45 Ma, West Philippine Basin floor, and Eocene–Early Oligocene arc volcanic debris shed from the proto-Izu–Bonin Mariana arc to the east. The basin basalts have trace element characteristics of MORB, and enrichments in Ba, Sr, Cs and Rb and $^{87}Sr/^{86}Sr$ result from mild post-eruptive alteration. Sr, Nd, Pb and Hf isotopic characteristics are similar to those of MORB-like West Philippine Basin basalts from other locations, and resemble Indian MORB more than Pacific MORB.

Volcanic clasts clearly have an island arc origin based on enrichment in LILE, and depletion in Ta and Nb relative to HFSE. The clasts also have low Hf/Sm, which, together with their isotopic composition, suggests that their mantle source incorporated a small amount of subducted sediment or sediment melt, together with fluids from the subducted Pacific plate. The geochemical characteristics of the arc volcanics, as well as the basement basalts, do not indicate that OIB sources were involved in their generation.

ACKNOWLEDGEMENTS

We thank Michael Bizimis for the help with the TIMS Pb and Hf isotope analysis at NHFM Isotope Lab at FSU, and Ilenia Arienzo and Valeria Di Renzo for their help with Sr and Nd analyses at Osservatorio Vesuviano, Napoli, Italy. Terry Plank and Katie Kelly hosted the first author and helped with the ICP-MS trace element analysis at Boston University. Thorough and constructive reviews by Jim Gill, Rob Stern, Sherman Bloomer, Marjorie Wilson and Richard Arculus significantly improved earlier versions of the manuscript. We also thank Alastair Lumsden for excellent editorial comments. This study was funded by NSF-POWRE (OCE 0074868 and OCE 0201602) and MARGINS (OCE 0001826) grants to R.H.V. and by JOI/USSAC postcruise science support grant to I.P.S. This research used samples and/or data provided by the Ocean Drilling Program. ODP is sponsored by the US National Science Foundation (NSF) and participating countries under the management of Joint Oceanographic Institutions (JOI), Inc.

REFERENCES

Arculus, R. J., Gill, J. B., Cambray, H., Chen, W. & Stern, R. J. (1995). Geochemical evolution of arc systems in the western Pacific: the ash and turbidite record recovered by drilling. In: Taylor, B. & Natland, J. (eds) *Active Margins and Marginal Basins of the Western Pacific. Geophysical Monograph, American Geophysical Union* **88**, 45–65.

Bizimis, M., Sen, G. & Salters, V. (2004). Hf–Nd isotope decoupling in the oceanic lithosphere: constraints from spinel peridotites from Oahu, Hawaii. *Earth and Planetary Science Letters* **217**, 43–58.

Cosca, M. A., Arculus, R. J., Pearce, J. A. & Mitchell J. G. (1998). $^{40}Ar/^{39}Ar$ and K/Ar age constraints for the inception and early evolution of the Izu–Bonin–Mariana arc system. *Island Arc* **7**, 579–595.

D'Antonio, M. & Kristensen, M. B. (2004). Hydrothermal alteration of oceanic crust in the West Philippine Sea Basin (Ocean Drilling Program Leg 195, Site 1201): inferences from a mineral chemistry investigation. *Mineralogy and Petrology* **83**, 87–112.

D'Antonio, M., Savov, I. P., Hickey-Vargas, R. & Leg 195 Scientific Party (2001). Petrology of igneous rocks cored at South Chamorro Seamount and West Philippine Sea, ODP Leg 195. 4th European ODP Forum, Tromsø, Norway, 10–12 April. *Norwegian Geological Society, Abstracts and Proceedings* **3**, 34.

Deschamps, A. & Lallemand, S. (2002). The West Philippine Basin: an Eocene to Early Oligocene back-arc basin opened between two opposed subduction zones. *Journal of Geophysical Research* **107**, 2322–2346.

Deschamps, A. & Lallemand, S. (2005). Geodynamic setting of Izu–Bonin–Mariana boninites. In: *Intra-Oceanic Subduction Systems. Geological Society, London, Special Publications* (in press).

Elliott, T. (2003). Tracers of the slab. In: Eiler, J. (ed.) *Inside the Subduction Factory. American Geophysical Union Monograph* **138**, 23–45.

Elliott, T., Plank, T., Zindler, A., White, W. M. & Bourdon, B. (1997). Element transport from subducted slab to juvenile crust at the Mariana Arc. *Journal of Geophysical Research* **102**, 14991–15019.

Fujioka, K., Okino, K., Kanamatsu, T., Ohara, Y., Ishisuka, O., Haraguchi, S. & Ishii, T. (1999). Enigmatic extinct spreading center in the Western Philippine backarc basin unveiled. *Geology* **27**, 1135–1138.

Gill, J. B., Hiscott, R. N. & Vidal, P. (1994). Turbidite geochemistry and evolution of Izu–Bonin arc and continents. *Lithos* **33**, 135–168.

Hall, R., Ali, J. R., Anderson, C. D. & Backer, S. J. (1995). Origin and motion history of the Philippine Sea Plate. *Tectonophysics* **251**, 229–250.

Hawkins, J. & Castillo, P. (1998). Early history of the Izu–Bonin–Mariana arc system: evidence from Belau and the Palau Trench. *Island Arc* **7**(3), 559–569.

Hickey-Vargas, R. (1989). Boninites and tholeiites from DSDP Hole 458, Mariana forearc. In: Crawford, A. J. (ed.) *Boninites*. London: Unwin Hyman, pp. 339–356.

Hickey-Vargas, R. (1991). Isotope characteristics of submarine lavas from the Philippine Sea: implications for the origin of arc and basin

Downloaded from http://petrology.oxfordjournals.org/ at Kainan University on March 28, 2015

magmas of the Philippine Sea plate. *Earth and Planetary Science Letters* **107**, 290–304.

Hickey-Vargas, R. (1998*a*). Geochemical characteristics of ocean island basalts from the West Philippine basin: implications for the sources of Southeast Asian plate margin and intraplate basalts. In: Flower, M., Chung, S.-L., Lo, C. H. & Lee, T.-Y. (eds) *Mantle Dynamics and Plate Interactions in East Asia. Geodynamics Series Monograph, American Geophysical Union* **27**, 365–384.

Hickey-Vargas, R. (1998*b*). Origin of the Indian Ocean-type isotopic signature in basalts from the West Philippine Sea plate spreading centers: an assessment of local vs large scale processes. *Journal of Geophysical Research* **103**, 20963–20979.

Hickey-Vargas, R. & Reagan, M. K. (1987). Temporal variation of isotope and rare earth element abundances in volcanic rocks from Guam: implications for the evolution of the Mariana arc. *Contributions to Mineralogy and Petrology* **97**, 497–508.

Hickey-Vargas, R., Hergt, J. M. & Spadea, P. (1995). The Indian Ocean-type isotopic signature in West Pacific marginal basins: origin and significance. In: Taylor, B. & Natland, J. (eds) *Active Margins and Marginal Basins of the Western Pacific*. *Geophysical Monograph, American Geophysical Union* **88**, 175–197.

Hickey-Vargas, R., Savov, I. P., Bizimis, M., Okino, K., Fujioka, K. & Ishii, T. (2005). Origin of diverse geochemical signatures in igneous rocks from the West Philippine Basin: implications for tectonic models. *American Geophysical Union Monograph* (in press).

Hilde, T. W. C. & Lee, C.-S. (1984). Origin and evolution of the West Philippine Basin: a new interpretation. *Tectonophysics* **102**, 85–104.

Hussong, D. M. & Uyeda, S. (1981). Tectonic processes and the history of the Mariana Arc, a synthesis of the results of the Deep Sea Drilling Project, Leg 60. In: Hussong, D. M., Uyeda, S., *et al.* (eds), *Initial Reports of the Deep Sea Drilling Project, 60*. Washington, DC: US Government Printing Office, pp. 909–929.

Johnson, M. C. & Plank, T. (1999). Dehydration and melting experiments constrain the fate of subducted sediments. *Geochemistry, Geophysics, Geosystems* **1**, 1999GC000014 (www.g-cubed.org).

Kelley, K. A., Plank, T., Ludden, J. & Staudigel, H. (2003). Composition of altered oceanic crust at ODP Sites 801 and 1149. *Geochemistry, Geophysics, Geosystems* **4**(6), 2002GC000435 (www.g-cubed.org).

Langmuir, C. H., Klein, E. & Plank, T. (1992). Petrological systematics of mid-ocean ridge basalts: constraints on melt generation beneath ocean ridges. In: Phipps Morgan, J., Blackman, D. K. & Sinton, J. M. (eds) *Mantle Flow and Melt Generation at Mid-Ocean Ridges*. *Geophysical Monograph, American Geophysical Union* **71**, 183–280.

Le Bas, M. J., Le Maitre, R. W., Streckeisen, A. & Zanettin, B. (1986). A chemical classification of volcanic rocks based on the total alkali–silica diagram. *Journal of Petrology* **27**, 745–750.

Macpherson, C. G. & Hall, R. (2001). Tectonic setting of Eocene boninite magmatism in the Izu–Bonin–Mariana forearc. *Earth and Planetary Science Letters* **186**, 215–230.

Marsh, N. G., Saunders, A. D. Tarney, J. & Dick, H. (1980). Geochemistry of basalts from the Shikoku and Daito basins, Deep Sea Drilling Project Leg 58. In: deVries, G., Klein, K., Kobayashi, K., *et al.* (eds) *Initial Reports, Deep Sea Drilling Project, 58*. Washington, DC: US Government Printing Office, pp. 805–842.

Mattey, D. P. Marsh, N. G. & Tarney, J. (1981). The geochemistry, mineralogy and petrology of basalts from the West Philippine and Parece Vela Basins and from the Palau–Kyushu and West Mariana Ridges, Deep Sea Drilling Project Leg 59. In: Kroenke, L., Scott, R., *et al.* (eds) *Initial Reports Deep Sea Drilling Project, 59*. Washington, DC: US Government Printing Office, pp. 753–797.

Nakamura, N. (1974). Determination of REE, Ba, Fe, Mg, Na and K in carbonaceous and ordinary chondrites. *Geochimica et Cosmochimica Acta* **38**, 757–775.

Okino, K., Ohara, Y., Kasuga, S. & Kato, Y. (1999). The Philippine Sea: a new survey results reveal the structure and history of the marginal basins. *Geophysical Research Letters* **26**, 2287–2290.

Pearce, J. A., Thirlwall, M. F., Ingram, G., Murton, B. J., Arculus, R. J. & van der Laan, S. R. (1992). Isotopic evidence for the origin of boninites and related rocks drilled in the Izu–Bonin (Osagawara) forearc, Leg 125. In: Fryer, P., Pearce, J. A., Stokking, L. B., *et al.* (eds) *Proceedings of the Ocean Drilling Program, Scientific Results, 125*. College Station, TX: Ocean Drilling Program, pp. 487–507.

Pearce, J. A., Kempton, P. D., Nowell, G. M. & Noble, S. R. (1999). Hf–Nd element and isotope perspective on the nature and provenance of mantle and subduction components in Western Pacific arc–basin systems. *Journal of Petrology* **40**, 1579–1611.

Plank, T. & Langmuir, C. H. (1998). The chemical composition of subducted sediment and its consequences for the crust and mantle. *Chemical Geology* **145**, 325–394.

Prinkney, D. R., Gill, J. & Williams, R.W. (2002). Hf isotopes and concentration anomalies in the Izu arc. *EOS Transactions, American Geophysical Union* **83**(T72A-1246), F1322.

Reagan, M. K., Hickey-Vargas, R. & Hanan, B. (2002) Evolution of IBM arc outputs. NSF MARGINS/IFREE Workshop on the Izu–Bonin–Mariana Subduction System, Honolulu, Hawaii, 8–13 September. http://www.margins.wustl.edu/SF/I-B-M/IZUBonin.html.

Salisbury, M. H., Shinohara, M., Richter, C., *et al.* (eds) (2002). *Proceedings of the Ocean Drilling Program, Initial Reports, 195*. College Station, TX: Ocean Drilling Program [CD-ROM].

Savov, I. P., Hickey-Vargas, R., Ryan, J. G. & D'Antonio, M. (2001). Pb isotope ratios in basalts from the West Philippine Backarc Basin, Leg 195, Site 1201D. *EOS Transactions, American Geophysical Union* **82**, 47.

Seno, T. & Maruyama, S. (1984). Paleogeographic reconstruction and motion history of the Philippine Sea. *Tectonophysics* **102**, 53–84.

Shipboard Scientific Party (2002). Site 1201. In: Salisbury, M. H., Shinohara, M., Richter, C., *et al.* (eds) *Proceedings of the Ocean Drilling Program, Initial Reports, 195*. College Station, TX: Ocean Drilling Program [CD-ROM].

Stern, R. J. (2004). Subduction initiation: spontaneous and induced. *Earth and Planetary Science Letters* **226**, 275–292.

Stern, R., Morris, J., Bloomer, S. & Hawkins, J. (1991). The source of the subduction component in convergent margin magmas: trace element and radiogenic isotope evidence from Eocene boninites, Mariana forearc. *Geochimica et Cosmochimica Acta* **55**, 1467–1481.

Stern, R. J., Fouch, M. J. & Klemperer, S. (2003). An overview of the Izu–Bonin–Mariana Subduction Factory. In: Eiler, J. (ed.) *Inside the Subduction Factory*. *American Geophysical Union Monograph* **138**, 175–222.

Stolper, E. & Newman, S. (1994). The role of water in the petrogenesis of Mariana Trough magmas. *Earth and Planetary Science Letters* **121**, 293–325.

Straub, S. (1997). Multiple sources of Quaternary tephra layers in the Mariana Trough. *Journal of Volcanology and Geothermal Research* **76**, 251–276.

Sun, S. S. & McDonough, W. F. (1989). Chemical and isotopic systematics of oceanic basalts: implications for mantle composition and processes. In: Saunders, A. S. & Norrey, M. J. (eds) *Magmatism in the Ocean Basins*. *Geological Society, London, Special Publications* **42**, 313–346.

Taylor, B. (1992). Rifting and the volcanic–tectonic evolution of the Izu–Bonin–Mariana arc. In: Taylor, B., Fujioka, K., *et al.* (eds)

Downloaded from http://petrology.oxfordjournals.org/ at Kainan University on March 28, 2015

Proceedings of the Ocean Drilling Program, Scintific Results, 126. College Station, TX: Ocean Drilling Program, pp. 627–651.

Todt, W., Cliff, R. A., Hanser, A. & Hofmann, A. W. (1993). Recalibration of NBS lead standards using a $^{202}Pb + {}^{205}Pb$ double spike. *Terra Abstracts* **5**, 396.

Uyeda, S. & Ben Avraham, Z. (1972). Origin and development of the Philippine Sea. *Nature* **240**, 176–178.

Wood, D. A. (1979). A variably veined suboceanic upper mantle—genetic significance for mid-ocean ridge basalts from geochemical evidence. *Geology* **7**, 499–503.

Woodhead, J. D., Hergt, J. M., Davidson, J. P. & Eggins, S. M. (2001). Hafnium isotope evidence for 'conservative' element mobility during subduction zone processes. *Earth and Planetary Science Letters* **192**, 331–346.

Downloaded from http://petrology.oxfordjournals.org/ at Kainan University on March 28, 2015